

Forest-floor respiration, N₂O, and CH₄ fluxes in a subalpine spruce forest: Drivers and annual budgets

Luana Krebs¹, Susanne Burri¹, Iris Feigenwinter¹, Mana Gharun², Philip Meier¹, Nina Buchmann¹

¹Department of Environmental Systems Science, Institute of Agricultural Sciences, ETH Zurich, Switzerland

5 ²Faculty of Geosciences, Institute of Landscape Ecology, University of Munster, Germany

Correspondence to: Luana Krebs (luana.krebs@usys.ethz.ch)

Abstract. Forest ecosystems play an important role in the global carbon (C) budget by sequestering a large fraction of anthropogenic carbon dioxide (CO₂) emissions and by acting as important methane (CH₄) sinks. The forest-floor greenhouse gas (GHG; CO₂, CH₄ and nitrous oxide N₂O) flux, i.e., from soil and understory vegetation, is one of the major components to consider when determining the C or GHG budget of forests. Although winter fluxes are essential to determine the annual C budget, only very few studies have examined long-term, year-round forest-floor GHG fluxes. Thus, we aimed to i) quantify seasonal and annual variations of forest-floor GHG fluxes; ii) evaluate their drivers, including the effects of snow cover, timing, and amount of snowmelt, and iii) calculate annual budgets of forest-floor ~~C and~~ GHG fluxes for a subalpine spruce forest in Switzerland. We measured GHG fluxes year-round during four years with four automatic large chambers at the ICOS Class 1 Ecosystem station Davos (CH-Dav). We applied random forest models to investigate environmental drivers and to gap-fill the flux time series. The forest floor emitted ~~23402336~~ g CO₂ m⁻² yr⁻¹ (average over four years). Annual and seasonal forest-floor respiration responded most strongly to soil temperature and snow depth. No response of forest-floor respiration to leaf area index or photosynthetic photon flux density was observed, suggesting a strong direct control of soil environmental factors and a weak or even lacking indirect control of canopy biology. Furthermore, the forest-floor was a consistent CH₄ sink (-0.71 g CH₄ m⁻² yr⁻¹), with annual fluxes driven mainly by snow depth. Winter CO₂ fluxes were less important for the CO₂ budget (6.0–7.3 %), while winter CH₄ fluxes contributed substantially to the annual CH₄ budget (14.4–18.4 %). N₂O fluxes were very low (0.007 g N₂O m⁻² yr⁻¹), negligible for the forest-floor GHG budget at our site. In 2022, the warmest year on record with below-average precipitation at the Davos site, we observed a substantial increase in forest-floor respiration compared to other years. The mean forest-floor ~~GHG~~ budget indicated emissions of ~~23172319~~±200 g CO₂-eq m⁻² yr⁻¹ (mean ± standard deviation over ~~four~~all years), with respiration fluxes dominating and CH₄ offsetting a very small proportion (0.8 %) of the ~~budget~~CO₂ emissions. Due to the relevance of snow cover, we recommend year-round measurements of GHG fluxes with high temporal resolution. In a future with increasing temperatures and less snow cover due to climate change, we expect increased forest-floor respiration at this subalpine site, ~~with negative effects on its~~ modulating the carbon sink capacity of the forest ecosystem.

30 **1 Introduction**

Carbon dioxide (CO₂), methane (CH₄), and nitrous oxide (N₂O) are the three main greenhouse gases (GHGs) driving global warming. Forest ecosystems play an important role in the global carbon (C) cycle by sequestering a large fraction of anthropogenic CO₂ emissions and by acting as an important CH₄ sink (Borken et al., 2006; Ni and Groffman, 2018; Friedlingstein et al., 2023). The GHG flux of the forest-floor, i.e., soil and understory vegetation, is one of the major
35 components to consider when determining the C budget of forests, since soil respiration is the second largest terrestrial C flux and accounts for approximately 70 % of CO₂ losses in temperate forests (IPCC, 2021; Yuste et al., 2005). However, how forest-floor GHG fluxes will respond to climate change is still largely unknown.

Global warming particularly affects high latitude and high altitude forests (IPCC, 2021), altering snowfall, length and timing of snow cover as well as melting and soil freeze-thaw cycles (CH2018, 2018; Klein et al., 2016). Nevertheless, there have been
40 very few studies that examined continuous, year-round and long-term forest-floor GHG fluxes in high latitude or high altitude forests (Barba et al., 2019; Luo et al., 2011). Unfortunately, measurements during periods with snow cover are challenging and thus often lacking due to logistical reasons, leading to winter fluxes missing even from multi-year studies (e.g., Richardson et al., 2019).

Forest-floor CO₂ fluxes include photosynthetic CO₂ uptake by plants as well as autotrophic and heterotrophic respiratory losses
45 from plants and soils, respectively (Hanson et al., 2000). All three processes and their contributions to the total soil CO₂ fluxes depend on biotic and abiotic factors as well as their interactions. For example, soil respiration is coupled to canopy photosynthesis and thus to incoming radiation, but also strongly controlled by soil conditions (i.e., soil temperature and moisture), substrate availability, and the microbial community (e.g., Högberg et al., 2001; Janssens et al., 2001; Scott-Denton et al., 2006). Furthermore, winter dynamics can impact soil respiration rates through changes in snow cover, soil freezing and
50 thawing cycles (Reinmann and Templer, 2018; Schindlbacher et al., 2007). Especially, freeze-thaw events have recently been the focus of research because they cause abrupt changes in biophysical soil conditions which can alter autotrophic and heterotrophic soil respiration rates (Song et al., 2017). How soil respiration responds to climate change is, however, not fully clear. With increasing soil temperatures as a consequence of increasing air temperatures (Lembrechts et al., 2022), global observations and models show a globally rising trend of soil respiration over recent decades and a continuation of the increase
55 with progressing climate change (Bond-Lamberty et al., 2018; Nissan et al., 2023). At the same time, there is evidence for a thermal optimum of ecosystem respiration over a range of different biomes, indicating a non-monotonic relationship between soil temperature and respiration (Chen et al., 2023).

Forest soils have been shown to act as an atmospheric CH₄ sink (Dutaur and Verchot, 2007). The uptake of CH₄ in well-aerated soils is related to the presence of methane-oxidizing bacteria (Saunois et al., 2020). This process is highly dependent on
60 environmental factors, including soil temperature (T_{soil}), soil texture (transport of CH₄ into the soil), soil moisture (transport of CH₄ into the soil and limitation of bacterial activity), and soil nitrogen (N) content (Borken et al., 2006; Luo et al., 2013; Ni and Groffman, 2018). Furthermore, biotic factors such as plant cover can affect CH₄ uptake of the forest floor through the

presence of *Sphagnum* moss species which are inhabited by methane-oxidizing bacteria (Basiliko et al., 2004). Generally, in temperate forests, CH₄ uptake increases in warmer and drier soils (Borken et al., 2006; Ni and Groffman, 2018). Winter dynamics further impact CH₄ fluxes, with frozen soil and snow cover affecting microbial activity and gas transport (Blankinship et al., 2018; Borken et al., 2006). Understanding the drivers of forest-floor CH₄ fluxes, including the complex interplay between biotic and abiotic factors, is vital for accurately modeling and predicting the role of forest ecosystems in the global CH₄ cycle.

Moreover, the forest-floor can act as a source or sink of N₂O (Chapuis-Lardy et al., 2007; Goldberg et al., 2010). Soil temperature, soil moisture, and N availability significantly influence N₂O fluxes through regulating microbial processes which are mainly responsible for N₂O production in soils, i.e., nitrification and denitrification (Schaufler et al., 2010). High N₂O emission rates in temperate forests have been found under warm and moist conditions (Luo et al., 2013). Furthermore, high N₂O emissions occur during freezing-thawing cycles and rewetting events, when abrupt changes in temperature and moisture conditions promote microbial activity and thus the release of N₂O (Goldberg et al., 2010; Papen and Butterbach-Bahl, 1999; Liu et al., 2018; Butterbach-Bahl et al., 2013). Understanding the dynamics of these processes and drivers, particularly during freezing-thawing cycles, is crucial for estimating N₂O emissions from forests.

In this study, we investigated combined measurements of forest-floor respiration, CH₄ and N₂O fluxes in a subalpine Norway spruce forest (Davos, CH-Dav, ICOS Class 1 Ecosystem station), in response to biotic and environmental drivers, based on four years of year-round measurements (2017, 2020-2022). Our objectives were to i) quantify seasonal and annual variations in climate variables and forest-floor respiration, CH₄ and N₂O fluxes; ii) evaluate the drivers of forest-floor GHG fluxes, including effects of snow cover, timing and amount of snowmelt; and iii) calculate the annual budgets of forest floor GHG fluxes. We hypothesized that the forest floor is a source of CO₂ throughout the years, with large seasonal variability due to the temperature sensitivity of respiratory processes, but very low N₂O emissions due to the overall low N supply at the site. In contrast, we expected that the forest floor is a net sink of CH₄, with soil temperature and snow dynamics being important drivers due to their impact on microbial activity and diffusion rates between soil and atmosphere. Thus, we expected the highest respiratory fluxes and CH₄ uptake in 2022, an exceptionally warm year at our site. Overall, we anticipated the forest-floor GHG budget being mainly determined by respiration fluxes, with CH₄ uptake only slightly offsetting the respiratory CO₂ losses and N₂O emissions being negligible.

2 Methods

90 2.1 Study site

The study site is a subalpine evergreen coniferous forest, located in the eastern Swiss Alps at an altitude of 1640 m a.s.l. (Davos Seehornwald; CH-Dav; 46°48'55.2" N, 9°51'21.3" E). The total annual precipitation is 876 mm, and the mean annual temperature is 4.3 °C (1997–2022). The site is certified as ICOS (Integrated Carbon Observation System) Class 1 Ecosystem station for eddy-covariance flux measurements since 2019. The dominant species is Norway spruce (*Picea abies* (L.) Karst),

95 with an average tree height of 18 m (max. 35 m), and a mean tree age of approx. 100 years (with some trees reaching over 300 years). Understory vegetation covers about 30 % of the surface and is mainly composed of blueberry (*Vaccinium myrtillus* and *Vaccinium gaulterioides*) and mosses (*Sphagnum* sp. Ehrh. and *Hylocomium splendens*). CH-Dav is a sustainably managed forest according to the Swiss National Forest Protection Law (1876; Tschopp, 2012). The soil types are chromic cambisols (L, F, H layers with 1 cm, 2 cm, and 1.5 cm thickness, respectively; A, B(h), B(fe), B, and (B)Cv horizons with 0–4 cm, 4–12 cm, 100 12–45 cm, 45–70 cm, and > 70 cm depth, respectively) and rustic podzols (L, F, H layers with 1 cm, 3 cm, and 7 cm thickness, respectively; Ah, (A)E, Bfe, BCv, and (B)Cv horizons with 0–3 cm, 3–10 cm, 10–40 cm, 40–80 cm, and > 80 cm soil depth, respectively; FAO classification; Jörg, 2008). Soil texture ranges from sand to sandy loam (Jörg, 2008). Soil bulk density at 5 cm depth of mineral soil is between 0.27–0.35 g cm⁻³ (Saby et al., 2023). Soil C and N stocks (0 to 60 cm depth) are on average 142.3 and 5.1 t ha⁻¹, respectively (Jörg, 2008).

105 2.2 Chamber flux measurements

2.2.1 Chamber set-up and tests

Forest-floor respiration, CH₄ and N₂O fluxes were measured during the years 2017 and 2020–2022 using a fully automated system with four chambers (FF1 to FF4), distributed within an area of 3600 m² in the forest to represent the eddy-covariance footprint. Concentrations of CO₂, CH₄ and N₂O were measured with a Dual Laser Trace Gas Analyzer (TILDAS, Aerodyne 110 Research, Billerica, USA) since 2017. To ensure high measurement quality, laser temperatures and tuning rates were adjusted on a regular basis. After the measurement campaign in 2017, the TILDAS was sent to Aerodyne for maintenance and repair (new N₂O laser source); measurements of all three GHG were resumed in fall 2019. In January 2021, the N₂O laser broke, thus N₂O measurements stopped. Since November 2019, CO₂ concentrations in the chambers were also measured with an infrared gas analyzer (LI-840, LI-COR Biosciences, Lincoln NE, USA). For the year 2020, CO₂ chamber measurements from both 115 TILDAS and LI-840 were available and used for further analyses (see below). For 2021 and 2022, only the IRGA CO₂ measurements were used.

Chambers were designed according to Brümmer et al. (2017), following the ICOS RI protocol for chamber measurements (Pavelka et al., 2018). The large opaque PVC chambers (white surfaces to increase albedo) rested on aluminum frames, and were inserted 10 cm into the soil, sealed with EPDM (ethylene propylene diene monomer) gaskets. Their large size (75 cm x 120 75 cm x 50 cm height, approx. 281 dm³) allowed to reduce edge effects as much as possible. Chambers were equipped with a pressure vent, as well as air temperature and pressure sensors (BME280, Bosch Sensortec GmbH, Reutlingen, Germany). During the winter periods with snowfall, extension frames (2 x 50 cm height) allowed to increase chamber height. A 17 Watt geared electric motor (80807021, Crouzet, Valence, France) was used to move the entire PVC chamber vertically and horizontally by about 190 cm and 70 cm, respectively (Fig. A.1). One webcam per chamber allowed remote observation of the 125 operation and estimates of snow cover and depth (see below). Since the vegetation inside the chamber frames was not cut, the chamber set-up measured forest-floor GHG fluxes (and not only soil fluxes). Due to their opaque material, no understory

photosynthesis was measured with the chambers. Soil and vegetation cover inside the chambers (differentiated into three plant functional types: moss, grass, blueberry) were assessed visually in June 2022, when also leaf area index (LAI) of the spruce forest was measured using digital photography above the chamber locations (Fuentes et al., 2008). One chamber cycle lasted 10 minutes, with 3 minutes for the actual measurement period (when chamber resided on the frame, i.e. was fully closed), 3.5 minutes for closing, and 3.5 minutes for opening the chambers (slow upward and sideward movement was controlled by an Arduino Ethernet). Thus, chambers were fully closed for 48 minutes per day (i.e., 3.3 % of the day), during which rainfall was fully excluded. If we added the time when the chambers were hovering directly over the frame (about 4 minutes per cycle), the chambers would be closed for a maximum of 7 minutes per chamber cycle (i.e., 7.8 % of the day). But this is a rather conservative estimate of rainfall exclusion, since rain does not always fallsfall vertically, and throughfall is typically much less than bulk precipitation due to canopy interception. Together with further tests on potential chamber effects, i.e., SWC inside vs. outside for two chambers and four years; T_{soil} inside vs. outside for four chambers and three years (see Appendix, Figs. A.2-4), we concluded that our chamber design and closure duration avoided potential effects on environmental conditions as much as possible.

During the 10 min cycles, concentrations were measured continuously once per second. The air from the chamber was fed to the gas analyzers in 6 mm OD tubing (Synflex 1300, Eaton, Dublin, Ireland) and pumped back to the chamber, forming a closed system. Tube lengths between chamber and instrument ranged between 49–85 m, and the flow rate ranged between 0.9–1.0 slpm. We determined the time lags for the arrival of gas in the instrument based on the change in chamber status (fully open, fully closed) and max. CO₂ concentrations measured. Switching of the air stream between different chambers and gas analyzers was accomplished using rotary selector valves (Valco Selectors, VICI AG International, Schenkon, Switzerland). Chamber cycles (lasting app. 1 h for four chambers) were repeated every three hours for each gas analyzer individually, leading to a total of 16 cycles per chamber and day (eight per gas analyzer). Leakage tests of all four chambers were performed in 2019. Variations caused by possible leakage were below 3% of the measured flux, as required by the ICOS RI protocol (Pavelka et al., 2018).

2.2.2 Data processing and quality assessment

The concentration increase in the chamber headspace over time was used to determine the respective flux F using Eq. (1):

$$F = \frac{\frac{\partial C}{\partial t} V \frac{m}{A} \frac{p}{V_m} \frac{T_0}{p_0} \frac{T}{T_0}}{m} \quad (1)$$

where $\frac{\partial C}{\partial t}$ is the concentration change over time ($\text{mol mol}^{-1} \text{s}^{-1}$), V the actual chamber volume (m^3), A the forest-floor area within the chamber frame (m^2), m the molecular mass (dimensionless), V_m the molar volume ($\text{m}^3 \text{mol}^{-1}$) of the respective gas, p the mean chamber pressure (Pa), p_0 the standard pressure (1013.25 Pa), T_0 the standard temperature (273.15 K), and T the mean chamber temperature (K). We accounted for the varying chamber volume due to snow depth and additional extension frames installed during winter. Thus, the actual chamber volume was calculated using Eq. (2):

$$V = A \times (h_{chamber} + h_{frame} - h_{snow}) \quad (2)$$

where $h_{chamber}$ is the height of the chamber, h_{frame} the height of the extension frame(s), and h_{snow} the snow depth. We fitted
160 a linear regression to the change in concentration of the respective gas over time ($\frac{\partial C}{\partial t}$) during the closed period of the chamber
(180 s), excluding the first 20 s after closing. The R^2 and root mean square error (RMSE) of the fit was later used for the quality
assessment and filtering of the calculated fluxes (see below). A positive flux means release from the forest floor to the
atmosphere, and a negative flux indicates uptake by the forest floor.

The quality of the calculated fluxes was ensured by removing negative CO₂ fluxes (Step 1), removing outliers (Step 2,
165 despiking), and applying a filter based on R^2 for CO₂ and CH₄ and based on root mean square error (RMSE) for N₂O (Step 3).
These three steps were applied to each GHG separately. In more detail: (1) We excluded negative CO₂ fluxes (about 2 % of
all fluxes). (2) We then despiked (i.e., removed outliers) the flux data set with a running mean algorithm using a width of 30
days. Step 2 removed 0.2 %, 0.7 % and 1.2 % of CO₂, CH₄ and N₂O fluxes, respectively. (3) For CO₂ and CH₄ fluxes, we
analyzed data separately for each gas, each chamber, as well as growing period (May to November) vs. dormant period
170 (December to April), and based the quality assessment on R^2 values. We removed fluxes with a R^2 value below the 10th
percentile of all R^2 values in the respective period (except if $R^2 > 0.9$), to avoid setting a fixed threshold for an acceptable R^2 .
The 10th percentile of R^2 values ranged from 0.21 to 0.99, being lower during the dormant compared to the growing period
(Tab. A.1). Step 3 excluded 6 % and 9 % of CO₂ and CH₄ fluxes, respectively. For N₂O fluxes, we separated data of the two
years available (2017, 2020) to account for the replacement of the N₂O laser source in 2019 and based the quality assessment
175 on the RMSE (due to the low magnitude of the N₂O fluxes). N₂O fluxes with an RMSE below the 10th percentile of all RMSE,
which were 0.13 and 0.03 for 2017 and 2020, respectively, were removed. Step 3 excluded 25 % of all N₂O fluxes. Furthermore,
for N₂O, we estimated a minimum reliable flux with the specifications of the TILDAS instrument (precision of 0.03 ppb) and
the closure time, i.e., any change of N₂O concentrations in the chamber headspace during the measurement period had to be >
0.06 ppb (McManus et al., 2006) or > 29.1 nmol N₂O m⁻² h⁻¹.
180 Overall, the initial time series consisted of 38'103 CO₂ (in 2020 from two gas analyzers), 27'503 CH₄ and 13'291 N₂O flux
measurements over the four years. After the quality checks described above, 34'938 CO₂ (92 %), 25'083 CH₄ (91 %), and
9'823 N₂O (74 %) flux measurements remained, which resulted in 4446, 3972, and 1755 daily means, respectively.

2.2.3 Static chamber measurements

In order to check for the validity of our N₂O flux measurements using the automatic chambers, we performed N₂O
185 measurements using static chambers (dimensions of $d = 30$ cm and $h = 30$ cm; Hutchinson and Mosier, 1981). We used eight
static chambers, i.e., four chambers next to the automatic chambers, and four chambers placed randomly within the research
area. Soil collars were installed two weeks prior to the first measurement campaign. Four rounds of measurements were done
on two days in October 2023 ($n=32$), when soil temperature was between 5.5-12 °C, well above the long-term mean, and when
WFPS at 5 cm depth were on average 13.1 %, favoring microbial activities. Three collars were irrigated between the first and
190 second measurement round on the two days to simulate a heavy rainfall event, favoring denitrification. We left the chambers

closed for 1 h and sampled air in the headspace every 20 min. Sampling and flux calculations were done as described in Barthel et al. (2022). All gas samples were analyzed at ETH Zurich for N₂O mole fraction using gas chromatography (456-GC, Scion Instruments, UK).

2.3 Environmental data

195 Each of the chambers had measurements of soil water content (SWC; EC-5, Decagon Devices Inc.) and T_{soil} (107, Campbell Scientific Ltd.) at 5 cm soil depth in close vicinity (< 2 m away from the chamber). To account for potential drivers of canopy photosynthesis modulating forest-floor fluxes, photosynthetic photon flux density (PPFD; PAR LITE, Kipp & Zonen), air temperature (TA; HygroClip HC2-S3, Rotronic AG), and precipitation (PREC; 1518H3, Lambrecht Meteo GmbH) data were used as well, measured at the tower above the tree canopy at 35 m height (precipitation measured at 25 m height).

200 We calculated water-filled pore space (WFPS) from the SWC measurements using Eq. (2):

$$WFPS = \frac{SWC}{1 - \frac{BD}{PD}} \times 100 \quad (2)$$

Bulk density (BD) was calculated using the data from a soil sampling campaign done in July 2018 according to ICOS RI standards (Arrouays et al., 2018; Saby et al., 2023). Soil data were used from soil profiles closest to the respective chambers (in total, data from six profiles were used). Particle density (PD) was assumed to be constant at 2.65 g cm⁻³ (Danielson and Sutherland, 2018). Mean daily snow cover and snow depth per chamber were derived from webcam images using a custom-made python image analysis tool, deriving snow depth from a scale installed in vicinity to each chamber within the image section.

2.4 Statistical analyses

2.4.1 Driver analysis

210 We used conditional random forests (RF) to model daily forest-floor respiration and CH₄ fluxes (based on all years and chambers) and investigated their environmental drivers. Due to the low N₂O fluxes, we excluded them from the RF analyses. We selected predictors which were known from the literature, i.e., daily averages of T_{air}, T_{soil} at 5 cm depth, WFPS at 5 cm depth, and PPFD as well as their one- and four-day leads (meaning that we shifted the variables forward in time by one and four days). Furthermore, we added snow depth and changes in snow depth from one day to another (Δ snow depth) to the predictor set. To account for factors which could explain differences in GHG fluxes among chambers, we included several chamber-specific characteristics (Tab. A.2), i.e., LAI, bare soil fraction in the chambers, and total C and N stocks in the topsoil (litter, organic layers, 0–20 cm depth of mineral soil). We applied the function *cforest* from the R-package “party” which can deal with highly correlated predictor variables (v1.3.10; Strobl et al., 2008, 2007). Prior to model development, predictors and target variables were centered and scaled using the “caret” *preProcess* function, which brings all variables and measurements from different sensors and locations into the same range, improving performance of the RF models (v6.0.93; Kuhn, 2008). The hyperparameter fitting was done using the *train* function from the R-package “caret” (see Appendix for final model set-up)

using 10-fold cross-validation. The assessment of driver importance in the RF model was done using the R package “permimp” which accounts for correlated variables within the predictor set (v.1.0.2; Strobl et al., 2007; Debeer and Strobl, 2020; Debeer et al., 2021). The calculated values for driver importance were rescaled to values between 0 and 1 using a min-max
225 normalization.

We developed RF models separately for daily CO₂ and CH₄ fluxes (N = 4446 and 3972, respectively). The training of the RF was done using only a fraction of the data set (70 %). The remaining 30 % of the data set was used as test dataset to evaluate model performance. Centering and scaling were done separately for training and test datasets to avoid data leakage. The performance of RF models was assessed using R² and RMSE. During model development, we tested several different predictor
230 sets. Furthermore, to optimize the models and to evaluate the robustness of model results, we evaluated the RF models trained on data sets separated by year of measurement or by chamber, and compared their accuracy to the model that was built using data from all years and all chambers. In total, 17 predictor variables entered the models (including the leads). RF models were also trained on seasonal data (i.e., spring, summer, autumn, winter; defined according to the meteorological definition) to investigate differences in drivers among seasons. For seasonal RFs, we used the same predictor sets as for the RFs developed
235 on the multi-year data set. We calculated partial dependence (PD) plots of conditional RFs using the “moreparty” package (v0.3.1; Robette, 2023) which is based on the “pdp” package (v0.8.1; Goldstein et al., 2015; Greenwell, 2017) to assess relationships between the four most important predictors and the predictions. The PD was calculated as the change in the average predicted value, while the predictor of interest was varied over its marginal distribution.

2.4.2 Flux gap-filling and budget calculations

240 The gap-filling of CO₂ and CH₄ fluxes was done using the RF models described above. Missing values in the predictor variables (gap length < 3 days) were linearly interpolated using the R package “chillR” (v0.72.8, Luedeling and Fernandez, 2022). The gap-filled flux data were then used to calculate annual budgets of forest-floor C fluxes per chamber. Since we estimated the annual forest-floor C budget for the study area, we reported the mean over the four chambers. To be able to compare CO₂, CH₄ and CH₄N₂O budgets, we converted ~~the CH₄ budgets and N₂O fluxes~~ into CO₂-equivalents (CO₂-eq) using the 100-year global warming potential of 27 for methane ~~of 27,~~ and 273 for N₂O (IPCC, 2021).
245

In addition, we modeled the daily forest-floor respiration fluxes using a Q₁₀ model according to Eq. (3):

$$R_S = R_{ref} \times Q_{10}^{\frac{T_{soil} - 10}{10}} \quad (3)$$

where R_{ref} is the modeled R_S at T_{soil} of 10°C, and Q₁₀ is the temperature sensitivity. We developed one model for the full dataset (all years and all four chambers together). The annual respiration budgets calculated with the Q₁₀ modeled fluxes were then
250 compared to the annual respiration budgets from the RF gap-filling. All statistical analyses were performed using R Statistical Software (v4.2.0, R Core Team, 2022).

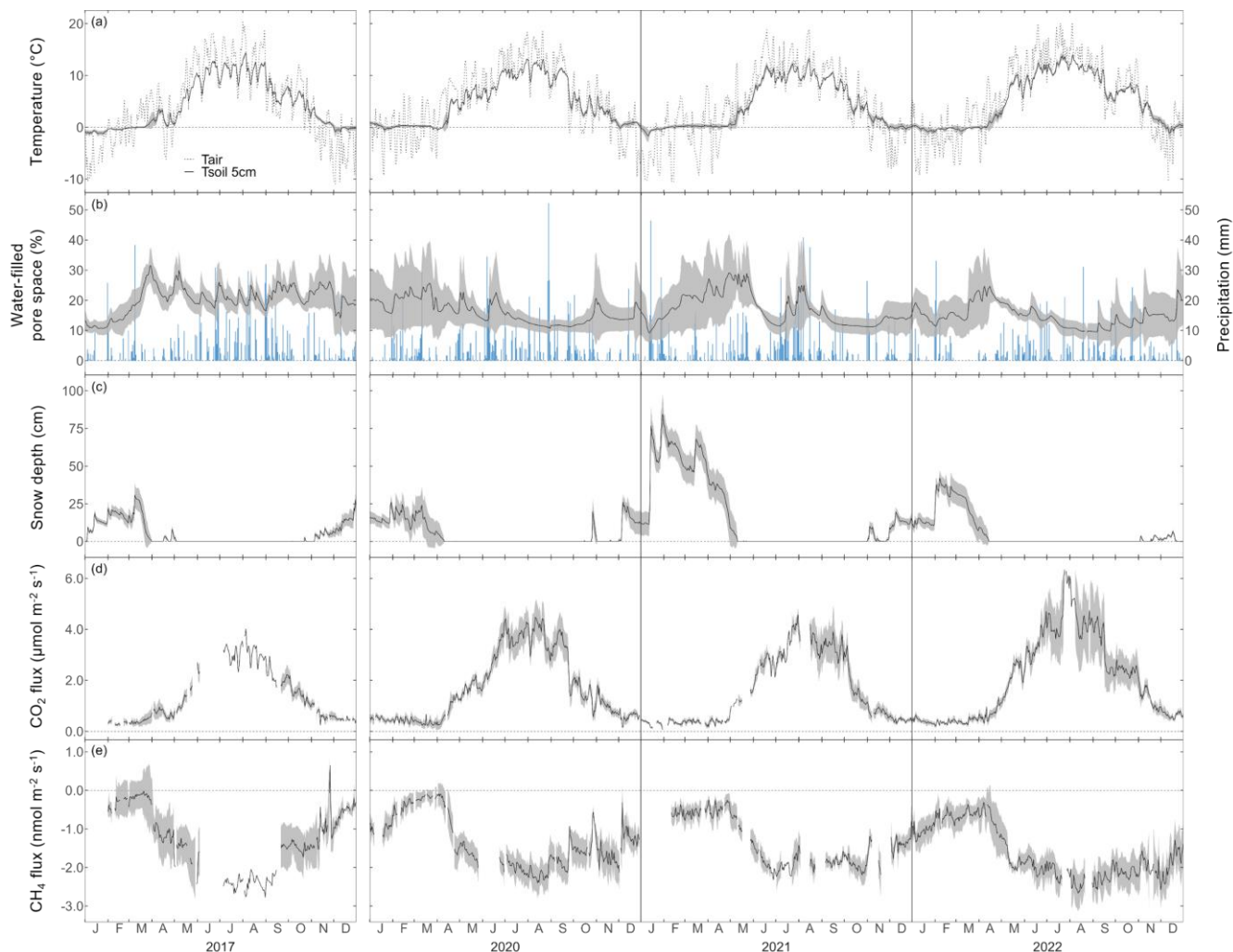
3 Results

3.1 Seasonal and interannual variability of environmental conditions and GHG fluxes

The seasonal courses of T_{air} and T_{soil} were very pronounced during the four years of the study, with highest temperatures in July and August, and lowest temperatures in January (Fig. 1a). All years showed highly variable WFPS with large differences among chambers (i.e., up to 35 % difference; Fig. 1b), and highest WFPS values during the snowmelt period, i.e., March to May. While the snow-covered periods usually started in November and lasted until April or May (Fig. 1c), the snow depths were much higher during winter 2020/2021 (reaching snow depths of over 1 m) compared to the other winters. Overall, the year 2022 was the warmest year ever recorded at the Davos research site so far, with an annual mean T_{air} of 5.6 °C (vs. the long-term mean of 4.3 °C; station data 1997–2022). Accordingly, annual mean T_{soil} at 5 cm was highest in 2022 for all chambers (annual mean T_{soil} over all chambers was 5.0 °C; Tab. A.2). At the same time, precipitation in 2022 was low (773 mm vs. long-term mean of 876 mm; station data 1997–2022), which led to comparably dry soil conditions (annual mean WFPS over all chambers was lowest in 2022 with 14.9 %).

The forest floor at the Davos Seehornwald site was a source of CO_2 during all four years, independent of the season (Fig. 1d). Typically, forest-floor respiration fluxes were very low in winter (mean CO_2 flux \pm standard deviation (SD): $0.46 \pm 0.14 \mu\text{mol m}^{-2} \text{s}^{-1}$), increased in spring after the snowmelt, and reached their maximum values in June to September (mean CO_2 flux over all years of $3.50 \pm 0.84 \mu\text{mol m}^{-2} \text{s}^{-1}$). Lowest forest-floor respiration was measured in January 2021 (min. CO_2 flux of $0.06 \mu\text{mol m}^{-2} \text{s}^{-1}$), highest respiratory fluxes were observed in July 2022 (max. CO_2 flux of $6.54 \mu\text{mol m}^{-2} \text{s}^{-1}$).

Moreover, the forest floor was a consistent sink for CH_4 , despite large short-term variations (days to weeks; Fig. 1e) and a few short peaks of CH_4 emissions in winter and spring. Seasonality of forest-floor CH_4 fluxes was very pronounced, with highest uptake in summer (mean CH_4 flux of $-2.11 \pm 0.28 \text{ nmol m}^{-2} \text{ s}^{-1}$), and still high CH_4 uptake rates during autumn and early winter (October to December; most clearly seen in 2022). With increasing duration of winter (January to March; Fig. 1e), the CH_4 sink strength decreased, with lowest CH_4 uptake measured in March (mean CH_4 flux of $-0.17 \pm 0.07 \text{ nmol m}^{-2} \text{ s}^{-1}$). However, after snowmelt, between April and end of May (depending on the year), CH_4 uptake rates increased sharply.



275

Fig. 1: Daily mean a) air temperature and soil temperature at 5 cm depth, b) water-filled pore space at 5 cm depth (left axis) and daily sum of precipitation (right axis), c) snow depth, and daily mean forest-floor d) respiration fluxes (not gap-filled), and e) CH₄ fluxes (not gap-filled), for the years 2017, 2020, 2021, and 2022. Please note the gap in measurements between 2017 and 2020. Black lines show means over four chambers, grey bands show standard deviations among four chambers. All data shown were quality-

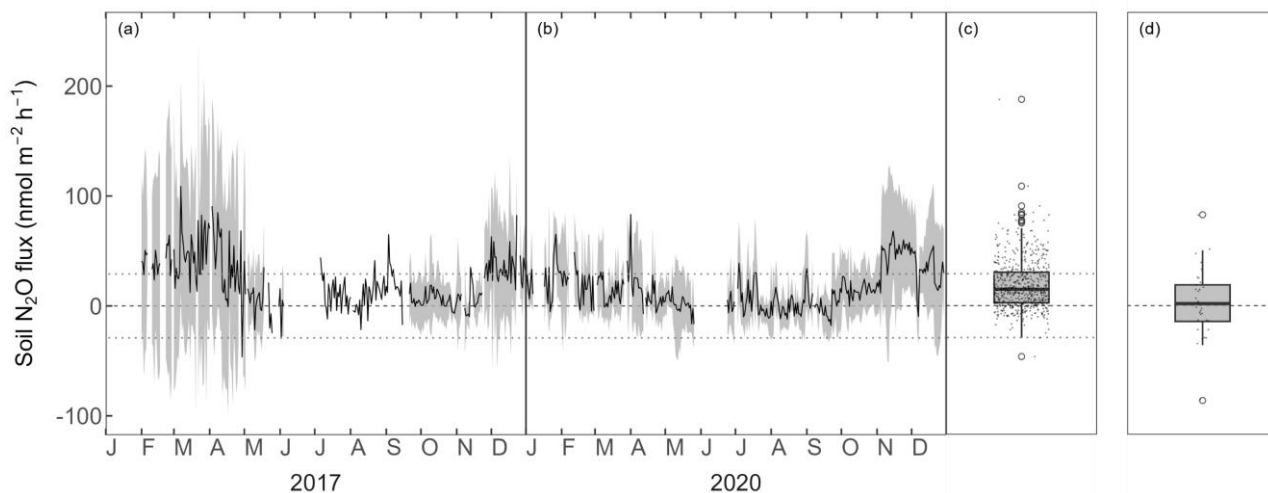
280 **checked as described in the main text.**

280

285

The forest floor N₂O fluxes ranged between -100–and 200 nmol m⁻² h⁻¹ but were mostly between 0 and 30 nmol m⁻² h⁻¹, with a mean over both years of 18.9±58.622.5 nmol N₂O m⁻² h⁻¹ (measured with automatic chambers and laser spectrometer; Fig. 2a, b, c). Winter fluxes (November to April) were generally higher and showed higher variability compared to the rest of the year. N₂O fluxes were within the calculated flux detection limit (29.1 nmol N₂O m⁻² h⁻¹) over a large part of the measurement period. N₂O fluxes measured manually with eight static chambers in October 2023 were low (mean ± SD = 2.9±31.1 nmol m⁻² h⁻¹).

$^2 \text{ h}^{-1}$, Fig. 2d) and agreed very well with the fluxes measured using the automatic chambers (mean in October: $10.2 \pm 14.7 \text{ nmol m}^{-2} \text{ h}^{-1}$). Both chamber measurements showed occasional N_2O uptake.



290 **Fig. 2: Forest-floor N_2O fluxes ($\text{nmol m}^{-2} \text{ h}^{-1}$) for the years a) 2017 and b) 2020. Black lines show means over four chambers, grey bands show standard deviations among four chambers. Boxplots show distribution of c) mean N_2O fluxes from four automatic chambers, and d) N_2O fluxes from static chamber measurements. The dotted lines depict the minimum flux ($29.1 \text{ nmol N}_2\text{O m}^{-2} \text{ h}^{-1}$) which could be detected by the Dual Quantum Cascade Laser spectrometer.**

295 3.2 Driver analyses with random forest models

The RF models captured the temporal dynamics and absolute magnitudes of the observed forest-floor respiration and CH_4 fluxes very well, with R^2 values of 0.95 and 0.87, respectively (relationships of observed vs. predicted fluxes from test datasets), and RSME of $0.32 \mu\text{mol m}^{-2} \text{ s}^{-1}$ and $0.27 \text{ nmol m}^{-2} \text{ s}^{-1}$, respectively (Fig. A.5). The seasonal RF models for forest-floor respiration fluxes yielded high R^2 values of 0.94, 0.73, 0.90 and 0.63 for spring, summer, autumn and winter, respectively
300 (Tab. A.3). Similarly, forest-floor CH_4 fluxes during spring, summer, autumn and winter were predicted well, with R^2 values of 0.80, 0.76, 0.72 and 0.73, respectively. Thus, the RF model performance was very good, also when shorter time periods were considered.

Forest-floor respiration fluxes combined for all four years and seasons were predominantly driven by T_{soil} at 5 cm depth: T_{soil} at the time of the flux measurements was the most important driver, but also T_{soil} with a four-day (second most important) and
305 with a one-day lead were relevant (Fig. 3). Furthermore, WFPS at 5 cm with a four-day lead played an important role. As expected, higher T_{soil} lead to higher respiration, while higher WFPS reduced forest-floor respiration. Drivers enhancing canopy photosynthesis, i.e., LAI or PPFD, did not play any role for forest-floor respiration. Separating forest-floor respiration fluxes into seasonal fluxes resulted in a clear distinction of drivers in winter compared to the other seasons (Fig. 3). Winter respiration

fluxes were mainly driven by snow depth (most important driver), leading to lower respiration fluxes with higher snow depths, while T_{soil} played a smaller role. As for the overall fluxes, summer forest-floor respiration fluxes were mainly driven by T_{soil} , increasing with T_{soil} . Also total N stocks were highly relevant in summer, with higher total N stock leading to lower respiration fluxes, much in contrast to the fluxes during spring and fall (Fig. 3).

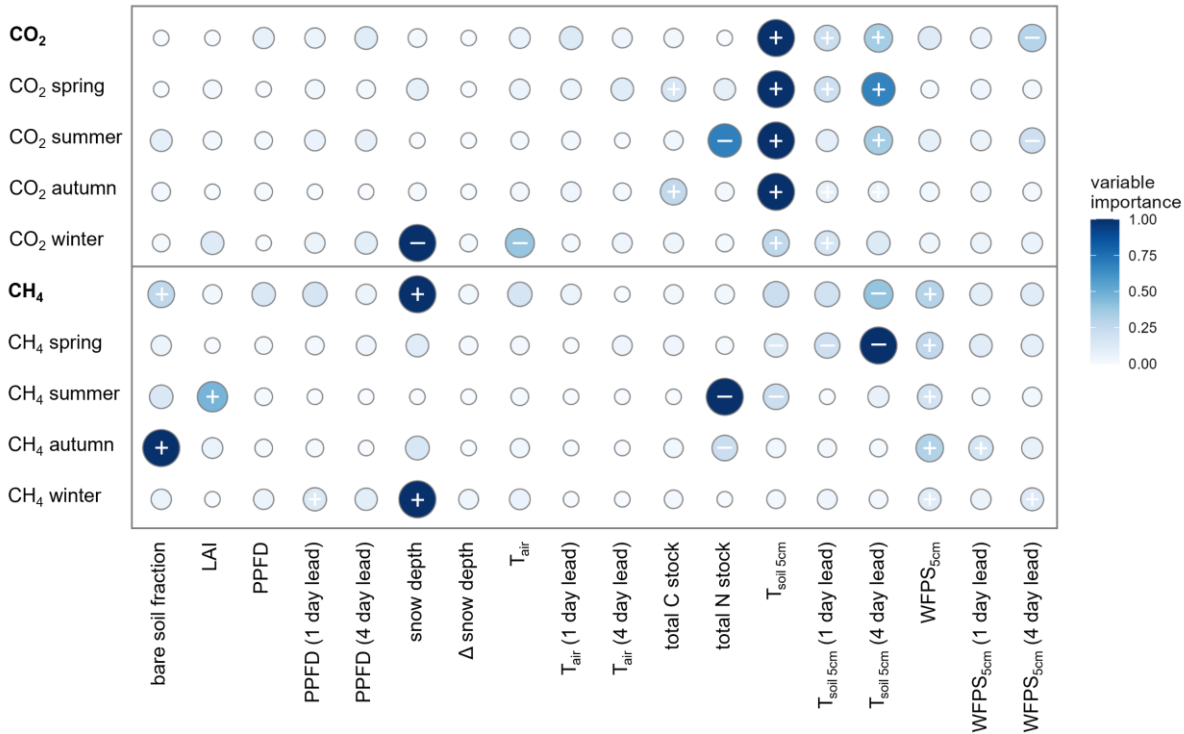
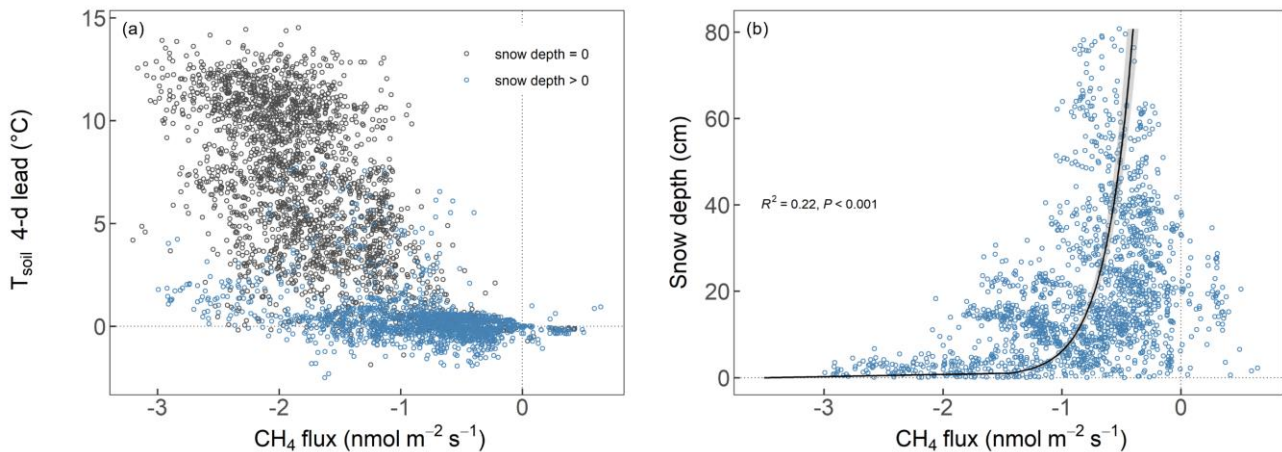


Fig. 3: Relative variable importance (rescaled to 0–1) according to the random forest driver analysis for forest-floor respiration (top; CO₂) and CH₄ (bottom) fluxes (not gap-filled; shown for the entire year, and per season). The direction of the effect of each predictor variable on the fluxes is shown by + (positive correlation) and - (negative correlation) signs, i.e., + indicates increased forest-floor respiration or decreased CH₄ uptake (i.e., increased CH₄ emissions). Signs are given for the four most important predictors which were investigated using partial dependence plots. See Materials and Methods for variable abbreviations.

The RF analysis showed that forest-floor CH₄ fluxes combined for all four years and seasons were mainly driven by the snow depth, with higher snow depths leading to more positive CH₄ fluxes and thus less CH₄ uptake (Fig. 3). Furthermore, the four-day lead of T_{soil} at 5 cm impacted the fluxes negatively, leading to increased CH₄ uptake, while WFPS at 5 cm and the bare soil fraction inside the chamber lead to strongly decreased CH₄ uptake. We found that the drivers of the forest-floor CH₄ fluxes changed profoundly among seasons. Spring CH₄ fluxes were mainly temperature-driven (higher temperatures leading to more CH₄ uptake). In summer, forest-floor CH₄ fluxes were mainly driven by total N stocks (higher N stocks leading to more

negative CH₄ fluxes and thus higher uptake) and by LAI (higher LAI leading to more positive CH₄ fluxes and thus lower uptake), reflecting spatial variability among chambers. In addition, CH₄ fluxes were influenced by an interaction of several drivers such as T_{soil} (higher T_{soil} leading to higher uptake) and WFPS (higher WFPS leading to lower uptake). For autumn CH₄ fluxes, bare soil fraction was the most important driver (more bare soil – and thus smaller moss cover (Tab. A.2) – leading to more positive CH₄ fluxes and thus less CH₄ uptake), but also WFPS played an important role. Winter CH₄ fluxes responded mainly to snow depth, with higher snow depth leading to less CH₄ uptake (Fig. 3). Closer investigation of the relationship between the two most important drivers (snow depth and the four-day lead of T_{soil}) with daily CH₄ uptake over the entire year revealed that the temperature dependence of the CH₄ fluxes disappeared when snow was present (Fig. 4a). We found a significant logarithmic relationship between CH₄ uptake and snow depths, showing a decrease in CH₄ uptake with increasing snow depth (Fig. 4b). Additionally, observations of CH₄ release were mainly attributed to snow covered periods (85 % of positive CH₄ fluxes). Furthermore, the Spearman correlation coefficient between the CH₄ fluxes in the months October to May and snow depth was high with $r = 0.59$.



340 **Fig. 4: Relationship between forest-floor CH₄ fluxes (nmol m⁻² s⁻¹, daily means per chamber) and a) 4-day lead of soil temperature at 5 cm depth (°C) and b) snow depth (cm) with the black line showing the fitted logarithmic curve.**

3.3 Forest-floor ~~C~~ and GHG budgets

345 The forest floor of this subalpine spruce forest was a source of CO₂ ~~and~~, a net sink of CH₄, and a close to zero N₂O source for all years of the study (averaged over all four chambers; Tab. 1). Mean annual ~~forest floor respiration and CH₄~~-budgets were 2336±200 g CO₂ m⁻² yr⁻¹ for forest-floor respiration, 0.007±0.009 g N₂O m⁻² yr⁻¹ for N₂O emissions (two-year mean), and -0.71±0.06 g CH₄ m⁻² yr⁻¹, respectively for CH₄ fluxes. The annual forest-floor respiration budgets were mainly determined by summer and early autumn fluxes (i.e., June to September). The interannual variability (SD) of forest-floor respiration budgets

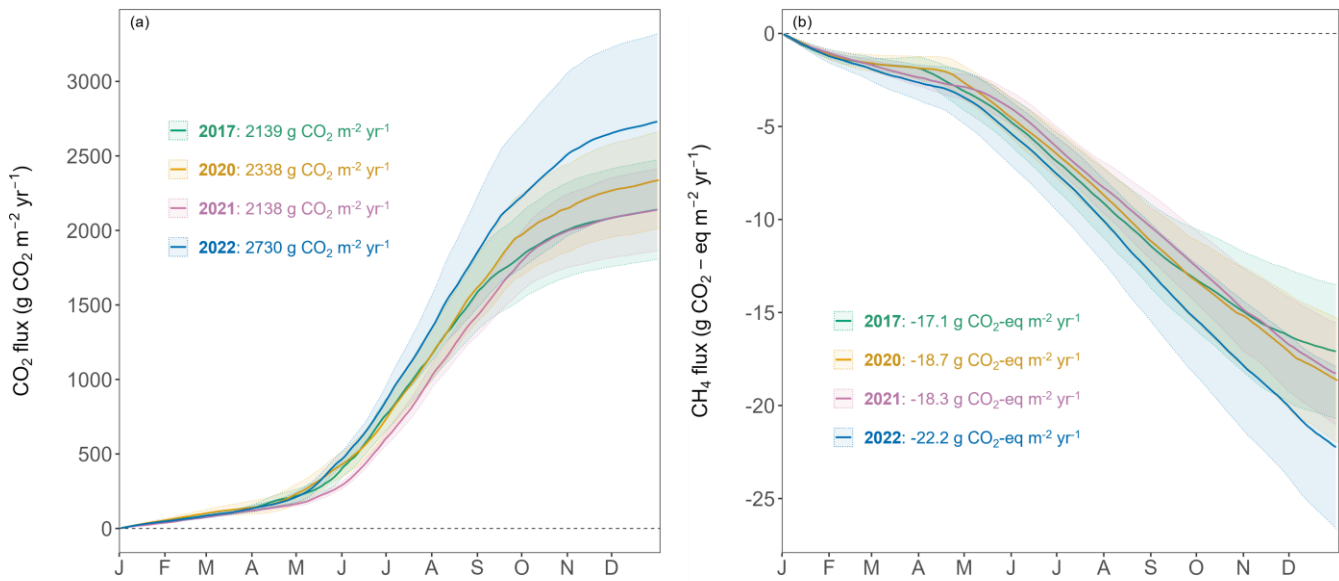
was approx. 200 g CO₂ m⁻² yr⁻¹ (8.6 %) during the four years of the study, with 2017 and 2021 showing smaller and 2022 the highest emissions. The annual forest-floor respiration budgets calculated with the Q₁₀ modeled data (2422±21 g CO₂ m⁻² yr⁻¹; Tab. 1, Fig. A.4) agreed well with the forest-floor respiration budgets based on the gap-filled fluxes using RF, also showing highest fluxes in 2022. A similar interannual variability (SD) as for the respiration budgets was found for the CH₄ budgets, with 8.5 % (0.06 g CH₄ m⁻² yr⁻¹). Comparing the magnitudes of ~~forest floor respiration and CH₄ budgets~~ all three GHG fluxes (in CO₂-eq) clearly showed that the respiration budget ~~determined~~ dominated the forest-floor ~~GHG~~ budget of the spruce forest, ~~since the~~ The forest floor CH₄ uptake (-19.1±1.8 g CO₂-eq m⁻² yr⁻¹) was about two orders of magnitude smaller than the respiration fluxes (2336±200 g CO₂-eq m⁻² yr⁻¹). ~~We did not develop an RF model for N₂O fluxes and did thus not calculate a forest floor N₂O budget based on gap filled fluxes. However, using the mean N₂O flux measured with the automatic chambers over two years (18.9 nmol m⁻² h⁻¹), we estimated the annual forest floor N₂O budget to be 0.007±0.025 g N₂O m⁻² yr⁻¹. Using the 100 year global warming potential of N₂O of 273 (IPCC, 2021) resulted in an annual forest floor N₂O budget of 1.99 g CO₂-eq m⁻² yr⁻¹, representing 0.09 % of the annual forest floor GHG budget (i.e., all three gases).~~ while the annual forest-floor N₂O emissions accounted for only 1.99±2.37 g CO₂-eq m⁻² yr⁻¹, representing 0.09% of the annual forest-floor GHG budget.

Tab. 1: Mean annual GHG budgets (±standard deviation (SD) over four chambers) of forest-floor respiration and CH₄ fluxes (using gap-filled data) and N₂O fluxes (mean of two years of measurements). The Q₁₀ budget was calculated with Eq. 3 (Q₁₀ and R_{ref} estimates were 4.8 and 3.16, respectively; overall R² was 0.86).

Year	Forest-floor respiration budget		Forest-floor CH ₄ budget		Forest-floor N ₂ O budget		Net <u>GHG</u> budget based on RF (g CO ₂ -eq m ⁻² yr ⁻¹)
	based on RF (g CO ₂ m ⁻² yr ⁻¹)	based on RF _{Q₁₀} (g <u>CO₂</u> m ⁻² yr ⁻¹)	based on Q₁₀ (g CO ₂ -eq m ⁻² yr ⁻¹)	(g <u>CO₂-eq</u> CH ₄ m ⁻² yr ⁻¹)	based on RF (g <u>CO₂-eq</u> m ⁻² yr ⁻¹)	(g <u>CH₄</u> N ₂ O m ⁻² yr ⁻¹)	
2017	2139±334	2407±28 <u>584±9</u> ±	-17.1±3.6 <u>2407±28</u>	47.1±3.6 <u>0.63±0.13</u>	0.47±0.10 <u>2.36±2.69</u>	0.63 <u>0.08±0.13</u> 0	2122±2124±334
2020	2338±324	2390±54 <u>638±8</u> 9	-18.7±3.3 <u>2390±54</u>	48.7±3.3 <u>0.69±0.12</u>	0.52±0.09 <u>1.66±2.00</u>	0.69 <u>0.06±0.12</u> 7	2319±2321±324
2021	2138±275	2204±40 <u>584±7</u> 5	-18.3±2.7 <u>2204±40</u>	48.3±2.7 <u>0.68±0.10</u>	-0.51±0.08	-0.68±0.10	2120±275
2022	2730±589	2687±40 <u>745±1</u> 6±	-22.2±4.4 <u>2687±40</u>	22.2±4.4 <u>0.82±0.16</u>	-0.62±0.12	-0.82±0.16	2708±579
Overall	2336±200	2422±21 <u>638±5</u> 5	-19.1±1.8 <u>2422±21</u>	49.1±1.8 <u>0.71±0.06</u>	0.53±0.05 <u>1.99±2.37</u>	0.71 <u>0.07±0.06</u> 9	2317±2319±200

The year 2022 can be considered an exceptional year, both in terms of annual forest-floor respiration and CH₄ fluxes (Tab. 1), but also in terms of temporal development (Fig. 5a). For CO₂, there were not only higher respiration rates in summer, but also a faster increase in respiration rates already in mid-April and sustained higher rates until later in the year (Fig. 5a). The

exceptionally high forest-floor respiration fluxes (2022 forest-floor respiration budget falls outside the 95% confidence interval = $\pm 1.96SD$, i.e., for the forest-floor respiration budget: $\pm 392 \text{ g CO}_2 \text{ m}^{-2} \text{ yr}^{-1}$) coincided with the higher-than-usual T_{soil} (annual mean T_{soil} of 2022 falls outside the 95% confidence interval) which was the main driver of spring, summer, and autumn forest-floor respiration fluxes. For CH_4 , we observed a higher annual CH_4 uptake in 2022 compared to other years (Tab. 1), mainly due to higher uptake rates in summer as well as still high uptake rates in autumn and early winter (Fig. 5b). Apart from higher T_{soil} driving the higher summer CH_4 uptake, this was mainly connected to comparably low soil moisture in autumn 2022 and the low snow depths in November and December 2022.



380 **Fig. 5: Cumulative forest-floor (a) respiration ($\text{g CO}_2 \text{ m}^{-2} \text{ yr}^{-1}$) and (b) CH_4 ($\text{g CO}_2\text{-eq m}^{-2} \text{ yr}^{-1}$) fluxes over four years. Lines show means of all four chambers; colored bands represent standard deviations among four chambers.**

4 Discussion

4.1 Interannual variability in forest-floor GHG fluxes

Over the four-year measurement period (2017 and 2020–2022), we collected high-resolution, reliable forest-floor GHG flux measurements for four very distinct years allowing comprehensive year-round analyses- (two years for N_2O). Notably, 2022 emerged as the warmest year ever recorded at the Davos site so far, coinciding with remarkably low precipitation and WFPS levels. The forest-floor respiration in 2022 exceeded those in the other three years by approximately 20%. Concurrently, we observed the highest forest-floor CH_4 uptake in 2022. It is well known that temperature is a major driver for any respiratory process (Davidson et al., 2006; Amthor, 2000). Also our RF driver analysis revealed that soil temperature was the main driver for forest-floor respiration fluxes, while no soil water limitation existed at this high elevation forest site during the study period.

Anjileli et al. (2021) reported that at multiple sites across the contiguous United States even during extreme heat events, soil respiration increased by approximately 25 % compared to average conditions, emphasizing the dominating influence of temperature on respiration also under extreme dry conditions for those sites. Additionally, Boroken et al. (2006) indicated that droughts can enhance the soil CH₄ sink in temperate forests. In contrast, the year 2021 was the coldest year among the four
395 years we investigated, with an annual mean T_{air} of 3.9 °C, mainly driven by below-average spring temperatures. This was reflected clearly in the ~~GHG~~forest-floor fluxes with below-average ~~forest-floor~~ respiration rates (approximately 30 % lower compared to the four-year mean) and below-average CH₄ uptake in spring 2021 (approximately 20 % lower compared to the four-year mean). Moreover, 2021 was an exceptional year in terms of snow depth, a relevant driver identified in this study (snow depth in winter and spring exceeded the four-year average by 87 % and 145 %, respectively).

400 While the year 2020 was also characterized by warm weather, its summer temperatures were less extreme than in 2022. Our findings revealed that the forest-floor respiration in 2020 did not reach the levels observed in 2022, supporting our driver analyses, clearly indicating that the exceptionally high summer temperatures experienced in 2022 were the primary driving force behind the 2022 annual forest-floor respiration fluxes. The RF models for 2022 resulted in slightly lower forest-floor respiration than measured, suggesting that no overfitting had occurred (Fig. A.6, A.7). Moreover, these results highlighted the
405 critical role played by extreme summer temperatures in shaping the C dynamics of this subalpine spruce ecosystem and underscored the significance of understanding their implications for future C budgets, potentially reducing the overall C sink capacity observed so far in this forest (Zielis et al., 2014).

We measured very low forest-floor N₂O fluxes which agreed well between the two measurement techniques used (automatic chambers and laser spectroscopy vs. static chambers and gas chromatography). Due to soil aeration and soil moisture
410 conditions at our site, we assumed that nitrification and not denitrification was the main process responsible for the N₂O emissions measured (Papen and Butterbach-Bahl, 1999; Butterbach-Bahl et al., 2013). At our site, N supply to plants and microorganisms is limited. Foliage N concentrations indicate N limitation for spruce (foliar N concentration are about 1 % in 0- and 1-yr-old needles as opposed to the optimum range of N content in needles between 1.5 and 2.3 %; Thimonier et al., 2010; Ingestad, 1959). Furthermore, N concentrations in the soil are low (1.4% in the organic layer, 0.4% in 10–20 cm depth; Jörg, 2008), ~~as well as~~ N deposition at the site (about 10 kg N ha⁻¹ yr⁻¹; Thimonier et al., 2019; Gharun et al., 2021). ~~Thus, our site is~~ corresponds to the lower level of critical N loads for forests in Switzerland (Hettelingh et al., 2017), well below the N deposition negatively related to basal area increments for spruce (20–22 kg N ha⁻¹ year⁻¹; Braun et al., 2017) or that with the highest positive effect on net ecosystem productivity, i.e., the C sink, of forests across Europe (22 kg N ha⁻¹ yr⁻¹; Wang et al., 2022). Thus, our site can clearly be considered rather low in N, which could be used for microbial transformations like
420 nitrification, competing with plant uptake (Schulze, 2000), therefore, low soil N₂O fluxes were to be expected. The observations of occasional low N₂O uptake measured with static and automatic chambers are in line with Goldberg and Gebauer (2009) who observed N₂O uptake in a German spruce forest. Microbial processes in forest soils can contribute to both uptake and release of N₂O, depending on the prevailing environmental conditions such as oxygen availability, soil moisture and microbial communities. Under anaerobic conditions, denitrification contributes to N₂O release, while under aerobic

425 conditions, N₂O reduction to N₂ can dominate over N₂O production, which results in observations of net N₂O uptake by soils
(Wen et al., 2017).

4.2 Drivers of forest-floor GHG fluxes

Forest-floor ~~GHG~~respiratory CO₂ and CH₄ fluxes were shown to have very distinct drivers across the different seasons.
430 Consistent with our expectations, soil temperature predominantly controlled forest-floor respiration fluxes, thereby influencing
the respiration budget at annual as well as seasonal scales (except winter season). In contrast, no effects of drivers known to
enhance canopy photosynthesis (i.e., LAI, PPFD) and thus below-ground allocation and soil respiration (Högberg et al., 2001)
were observed on the forest-floor respiration fluxes for any time in this spruce forest, suggesting a strong direct control of
environmental factors and only a weak or even lacking indirect control of canopy biology or structure. Drivers of forest-floor
435 CH₄ fluxes were much more variable compared to those of forest-floor respiration fluxes, with winter CH₄ fluxes being affected
by the same driver (snow depth) as the annual fluxes. The observations of lower CH₄ uptake during snow cover reflect the
results of Heinzle et al., 2023 from a long-term soil warming experiment in a temperate forest. The findings that snow depth
and WFPS (in autumn) were important drivers of forest-floor CH₄ fluxes supported the hypothesis proposed by Borken et al.
(2006), who emphasized the role of factors influencing the diffusion rates of atmospheric CH₄ into the soil, such as SWC and
440 snow cover, in determining CH₄ uptake in forest soils. Notably, previous studies had also reported a close relationship between
CH₄ fluxes and seasonal changes in soil moisture (Ni and Groffman, 2018; Ueyama et al., 2015). However, our results indicated
that in spring and summer, T_{soil} rather than WFPS played a more important role in driving forest-floor CH₄ uptake.
Additionally, we identified a notable influence of soil N on summer CH₄ fluxes, with higher N stocks, and thus most likely
higher N mineralization during the summer months, corresponding to enhanced CH₄ uptake. This aligned with previous
445 findings in forest ecosystems, where soil mineral N had been shown to stimulate CH₄ oxidation (Goldman et al., 1995;
Martinson et al., 2021). Moreover, we found a positive correlation between bare soil fraction and forest-floor CH₄ uptake, i.e.,
more bare soil and thus lower moss cover leading to lower forest-floor CH₄ uptake. This is in line with findings that *Sphagnum*
mosses can promote CH₄ oxidation (Basiliko et al., 2004). Also, for forest-floor CH₄ fluxes, hardly any effect of tree canopy
biology was detected (except for summer). Thus, a strong direct control of environmental factors on both forest-floor
450 respiration and CH₄ fluxes was observed, increasing the vulnerability of the forest C sink with future climate change (IPCC,
2021).

4.3 Forest-floor ~~C~~and GHG budgets

The overall forest-floor ~~GHG~~ budget (i.e., CO₂ and CH₄) showed a total emission of 23172319±200 g CO₂-eq m⁻² yr⁻¹,
dominated by the annual forest-floor respiration budget (2336±200 g CO₂ m⁻² yr⁻¹), which was within the range of studies
455 conducted in temperate, subalpine or boreal forests which we considered comparable to our site (1070–2906 g CO₂ m⁻² yr⁻¹;
Gaumont-Guay et al., 2014; Groffman et al., 2006; Schindlbacher et al., 2007, 2014; Wang et al., 2013; Xu et al., 2015). Also

our estimate of annual CH₄ budget at the site (-0.71±0.06 g CH₄ m⁻² yr⁻¹) fell within the range of -1.6 to -0.18 g CH₄ m⁻² yr⁻¹ observed in other forest studies (Borken et al., 2006; Luo et al., 2013; Ueyama et al., 2015; Yu et al., 2017), offsetting a mere 0.8 % of forest-floor respiration. Our estimate of the annual N₂O budget of 0.0073 g N₂O m⁻² yr⁻¹ agreed well with previous studies (Rütting et al., 2021; Ullah et al., 2009). For instance, a study conducted in a boreal spruce forest with low N deposition rates (about 5 kg N ha⁻¹ yr⁻¹) reported very low mean N₂O fluxes of around 0.0077 g N₂O m⁻² yr⁻¹ (Rütting et al., 2021). Higher soil N₂O emissions (0.08 g N₂O m⁻² yr⁻¹) have been observed in a temperate forest with higher N availability (N deposition rates 18 kg N ha⁻¹, N stocks in litter layer and mineral soil ~15 t ha⁻¹; Heinze et al., 2023). Winter fluxes contributed a large fraction to the overall CH₄ budget (14.4–18.4 %), but played a less important role for the forest-floor respiration budget (6.0–7.3 %), similar to the CO₂ contribution in other mid latitude and temperate ecosystems (5.5–8.9 %; Gao et al., 2018; Wang et al., 2013) but smaller than some high latitude and other subalpine ecosystems (12–20 %; Kim et al., 2017; Schindlbacher et al., 2007; Xu et al., 2015). To date, only a few studies have examined soil or forest-floor GHG fluxes in subalpine, temperate, or boreal forests, measuring CO₂, CH₄ and N₂O fluxes in parallel (Tab. 2). Tab. 2 includes studies examining fluxes from both the forest floor (soil and ground vegetation) and the soil. However, their comparability is constrained as forest-floor flux measurements encompass both soil respiration (including heterotrophic and root respiration) and autotrophic respiration from forest-floor plants, whereas soil flux measurements specifically capture soil respiration (Barba et al., 2018). It is noteworthy that the integration of year-round and temporally highly resolved measurements remains rather uncommon; to our knowledge, only two other studies with year-round measurements of CO₂, CH₄ and N₂O exist apart from the current study (Luo et al., 2011; Pilegaard et al., 2003). On the one hand, previous studies frequently measured fluxes for only a limited period of the year, often excluding the dormant season. On the other hand, many of the studies adopted a weekly to monthly measurement frequency, potentially missing the full range of flux magnitudes. If year-round measurements of forest-floor respiration are not feasible, using Q₁₀ models might be a viable option, as long as the annual temperature range is being well covered, as seen in the agreement between our respiration budget based on gap-filled continuous measurements and the Q₁₀ respiration budget. However, although T_{soil} was identified as the primary driver of forest-floor respiration, it was not the only driver. We argue that Q₁₀ models are not able to capture extreme respiration fluxes which might be caused by more drivers than temperature alone. Many studies have shown that Q₁₀ models do not reproduce measured fluxes well when additional drivers impact the fluxes, for instance when soil moisture, frost, or carbohydrate limitations come into play (e.g., Ruehr et al., 2010; Reichstein et al., 2013; Mitra et al., 2019). In contrast, our high-resolution dataset coupled with machine learning offered a more comprehensive approach, which included multiple environmental variables and at the same time was able to consider chamber-specific characteristics, and thus was able to capture the extreme fluxes we observed in summer 2022. Thus, we think that the reliability of the RF budget is higher than that of the Q₁₀ budget. Moreover, identifying important drivers for GHG fluxes is the more reliable, the longer and thus typically the more frequent measurements were done. Additionally, to effectively capture the dynamic nature of soil and/or forest-floor ~~GHG~~ fluxes, it is essential to use automatic chambers with high temporal resolution, preferentially opaque to exclusively quantify respiration. Therefore, we recommend continuous, year-round measurements to reliably estimate annual forest-floor ~~C~~ and GHG budgets, particularly when large seasonal variability of

potential drivers is expected, or when the duration of the active period, i.e., start and end of the snow-free period, is highly variable like in high elevation or high latitude ecosystems. Particularly with the anticipated impacts of future climate change (IPCC, 2021), duration of growing periods will change, and winter fluxes (or the lack thereof) will gain increasing importance (Xie et al., 2017).

495 **Tab. 2: Previously published studies investigating forest-floor or soil CO₂, CH₄ and N₂O fluxes in parallel in temperate, subalpine, or boreal forests using automatic or static chambers. n.a. = not available.**

Chamber method	Location	Forest type	Years	Duration	No. chambers	Frequency	Veg. in chambers	CO ₂ flux rates ($\mu\text{g CO}_2 \text{ m}^{-2} \text{ s}^{-1}$)	CH ₄ flux rates ($\text{ng CH}_4 \text{ m}^{-2} \text{ s}^{-1}$)	N ₂ O flux rates ($\text{ng N}_2\text{O m}^{-2} \text{ s}^{-1}$)	Reference
Automatic	46.82° N 9.86° E	Subalpine (spruce)	2017, 2020–2022	Year-round	4	3 h	Yes	74.1±6.3	-22.5±1.9	0.2±0.83	This study
Automatic	39.09° N 75.44° W	Temperate (mixed)	2017	Apr–Jul	3	1 h	No	362.6±24.2	-10.6±1.0	-2.0±0.5	Barba et al., 2019
Static	43.23° N 3.20° W	Radiata pine, Douglas fir, beech	2010–2011	Year-round	6	Biweekly	Yes	14.7±1.6	0.8±0.1	1.3±0.4	Barrena et al., 2013
Static	37.07° N 119.19° W	Montane mixed-conifer (Mediterranean-type climate)	2010–2012	Snow free period	24	Weekly–monthly	n.a.	51.7–63.3	-9.6–4.8	-0.3–1.7	Blankinship et al., 2018
Static	35.66° S 148.15° E	Temperate (eucalypt)	2006	2 weeks in Nov	10	4 h	No	90.4±1.9	-19.2±0.4	1.4±0.04	Fest et al., 2009
Static	43.93° N 71.75° W	Northern hardwood (beech, maple, birch)	1998–2000	Year-round	8	Weekly–monthly	n.a.	26.7–46.5	-20.0–7.9	2.0–7.0	Groffman et al., 2006
Static	42.40° N 128.10° E	Broad-leaved Korean pine mixed	2019	Mar–Oct	8	Twice a week–twice a month	n.a.	241.0±114.9	-35.9±12.5	9.7±6.2	Guo et al., 2020
Static	48.09° N 16.01° E	Temperate (beech)	1997	Apr–Nov	8	Biweekly	Yes	53.0–57.8	-5.6–3.2	11.9–30.5	Hahn et al., 2000
Static	43.83° N 74.87° W	Temperate (mixed)	2008	May–Jul	15	Biweekly	Yes	10.2–101.8	-16.7–42.1	-1.2–2.8	Hopfensperger et al., 2009
Static	47.03° N 8.72° E	subalpine (spruce)	2007–2012	Year-round	10	Every 3 weeks	Yes	48.8	-8.0–13.4	-1.2–2.9	Krause et al., 2013
Automatic (CO ₂), static (CH ₄ , N ₂ O)	48.50° N 11.17° E	Temperate (spruce)	1994–1997, 2000–2010	Year-round	5	1 h (CO ₂), 2 h (CH ₄ , N ₂ O)	n.a.	81.3–106.9	-14.8–3.8	1.0–14.9	Luo et al., 2011
Static	46.67–47.93° N 91.75–92.52° W	Boreal-temperate (mixed)	2013	May–Oct	48	Monthly	Yes	0.002–0.004	-0.0014–-0.0003	-10.3–10.3	Martins et al., 2017
Static	33.30–33.47° N 108.35–108.65° E	Temperate–cold temperate (deciduous broad-leaved & coniferous)	2012–2014	Year-round	60	Weekly–monthly	Yes	44.4–86.9	-24.0–3.8	5.9–11.2	Pang et al., 2023

Automatic (CO ₂), static (CH ₄ , N ₂ O)	55.48° N 11.63° E	Temperate (beech)	1998–1999, 2001	Year-round	5 (CO ₂), 6 (CH ₄ , N ₂ O)	2 h (CO ₂), biweekly (CH ₄ , N ₂ O)	Yes	n.a.	n.a.	n.a.	Pilegaard et al., 2003
Automatic	45.20° N 68.74° W	Sub-boreal (spruce, hemlock)	2013–2016	May–Nov	3-5	30 min	n.a.	n.a.	n.a.	n.a.	Richardson et al., 2019
Concentration profiles	41.33° N 106.33° W	Subalpine (spruce, fir)	1991–1992	Mar–May	2	Daily–biweekly	Yes	18.3–31.6	-0.0029–-0.0004	0.0003–0.0004	Sommerfeld et al., 1993
Static	49.26–52.20° N 74.03–76.07° W	Boreal (black spruce, jack pine, aspen, alder)	2007	May–Oct	48	Monthly	Yes	34.4–64.0	-6.7–1.6	0.4–0.8	Ullah et al., 2009
Static	57.13° N 14.75° E	Cold temperate (coniferous)	1999–2002	Year-round	30	Weekly–biweekly	Yes	28.5–60.2	0.0–50.7	1.0–2.9	Von Arnold et al., 2005
Static	53.28–53.50° N 122.10–122.45° E	Cold temperate continental monsoon	2016–2018	Year-round	9	Weekly–monthly	Yes	2.2–180.8	-15.9–9.0	-1.1–8.6	Wu et al., 2019

5 Conclusions

500 Forest-floor GHG fluxes, measured during multiple years with large opaque automatic chambers, were mainly driven by environmental factors, with only limited impacts of tree biology or structure. Particularly, in light of climate change-induced variations in the onset of the active growing season, growing season length, and winter conditions, we recommend to spatially expand the deployment of such chambers at research stations capable of year-round measurements, including periods with snow cover. Since our forest study site was very low in N supply and thus N₂O fluxes were very low, it remains to be seen
505 how large annual N₂O emissions are from other forest sites with higher N supply and what drivers are most relevant [there](#). As temperatures will continue to rise due to climate change, and warm and dry conditions such as in the recent summers are projected to become more frequent and more severe, we expect an increase in forest-floor respiration at the Davos spruce forest and similar subalpine or high latitude ecosystems. Similarly, anticipated milder winters with reduced snowfall, resulting in shorter snow cover duration and lower average snow depth, will likely contribute to enhanced forest-floor respiration and
510 increased forest-floor CH₄ uptake in the future. Since respiratory CO₂ losses are typically much larger than ~~the~~ CH₄ uptake [rates](#), as at our site, we expect the forest floor to become a more substantial C source in the future, potentially [reducing/modulating](#) the overall C sink capacity of this type of forest.

Data availability. The data used in this study will be made publicly available from the ETH Research Collection (<https://doi.org/10.3929/ethz-b-000619728>, preliminary link).

515 *Author contributions.* NB designed the study; PM, LK and SB conducted the field work; SB and LK processed the data; LK performed the data analyses, developed the models, and wrote the manuscript draft; SB, MG, PM, IF and NB commented on the manuscript and contributed substantially to discussions and revisions.

Competing interests. The authors declare that they have no conflict of interest.

520 *Acknowledgements.* The authors thank our colleagues Lutz Merbold, Matti Barthel, Lukas Hörtnagl, Thomas Baur, Werner Eugster and Liliana Scapucci for their assistance in designing and setting up the chambers, conducting fieldwork, and providing helpful inputs during the flux processing and data interpretation. Their contributions have greatly contributed to the progress of this study.

Financial support. This research has been supported by the Swiss National Science Foundation (SNSF), in the projects ICOS-CH Phase 1, 2, 3 (Grant-N° 20FI21_148992, 20FI20_173691, 20FI20_198227) and COCO (Grant-N° 200021_197357).

525

A Appendix

Tab. A.1: 10th percentiles of R² values from linear regressions used for flux calculations per gas, given separately for each chamber (FF1 to FF4) and growing and dormant periods. Percentiles were applied as quality thresholds.

Gas	Period	FF1	FF2	FF3	FF4
CO ₂	growing period	0.97	0.98	0.98	0.99
	dormant period	0.35	0.48	0.47	0.68
CH ₄	growing period	0.92	0.96	0.92	0.93
	dormant period	0.41	0.26	0.21	0.61

Tab. A.2: Site characteristics of the four chambers (FF1 to FF4). Annual means and standard deviations are shown for soil temperature (T_{soil}) and water filled pore space (WFPS) at 5 cm, mean and max snow depth, and days with snow cover. LAI, soil, and vegetation cover inside each chamber were determined in June 2022. Soil data (bulk density, pH, C and N stocks in the topsoil, i.e., litter, organic material layers, and 0–20 cm depth of mineral soil) were taken from Jörg (2008) and Saby et al. (2023).

Site characteristics	FF1	FF2	FF3	FF4	Mean
T_{soil} at 5cm (°C)					
2017	4.44 ± 4.67	4.16 ± 4.84	4.29 ± 4.86	4.56 ± 4.52	4.36 ± 0.17
2020	4.66 ± 4.32	4.40 ± 4.46	4.46 ± 4.34	4.87 ± 4.15	4.60 ± 0.22
2021	4.18 ± 4.25	3.80 ± 4.48	3.74 ± 4.84	4.26 ± 4.20	3.99 ± 0.26
2022	5.15 ± 4.70	4.83 ± 4.96	4.70 ± 5.38	5.18 ± 4.61	4.97 ± 0.24
WFPS at 5 cm (%)					
2017	20.1 ± 5.09	17.2 ± 4.30	21.3 ± 6.82	22.5 ± 7.42	20.3 ± 2.27
2020	15.9 ± 2.88	15.5 ± 3.85	9.8 ± 0.69	23.9 ± 9.55	16.3 ± 5.79
2021	16.8 ± 3.88	14.5 ± 3.88	11.8 ± 4.45	25.0 ± 10.5	17.0 ± 5.70
2022	15.1 ± 4.19	12.7 ± 3.27	10.4 ± 3.56	21.3 ± 7.16	14.9 ± 4.70
Max snow depth (cm)					
2017	34.7	40.7	27.4	25.6	47.4 ± 24.5
2020	31.8	41.7	25.9	22.0	58.6 ± 30.0
2021	83.9	103.0	79.5	62.6	43.5 ± 25.0
2022	39.4	48.7	41.1	36.8	36.8 ± 18.3
Mean snow depth (cm)					
2017	5.8 ± 8.4	6.4 ± 9.8	4.5 ± 6.4	3.9 ± 6.2	5.1 ± 1.2
2020	4.3 ± 7.0	8.6 ± 12.1	4.2 ± 7.0	3.5 ± 6.0	5.2 ± 2.3
2021	17.6 ± 25.0	22.2 ± 29.5	14.6 ± 22.7	14.8 ± 21.0	17.3 ± 3.6
2022	5.1 ± 9.3	8.3 ± 14.1	6.1 ± 11.7	4.9 ± 9.5	6.1 ± 1.6
Days with snow cover					
2017	152	159	152	148	153 ± 5
2020	126	142	123	117	127 ± 11
2021	172	189	161	169	173 ± 12
2022	138	145	134	132	137 ± 6
Leaf area index (LAI)	2.9	4.2	3.1	2.9	3.3 ± 0.6
Soil cover inside chamber (%)					
bare soil	0	50	70	0	30 ± 36
moss	90	50	20	90	63 ± 34
grass	5	1	0	0	2 ± 2

<i>Vaccinium</i>	60	0	10	30	25 ± 26
Bulk density at 5 cm of mineral soil (g cm ⁻³)	0.27	0.35	0.32	0.35	0.32 ± 0.04
pH	2.8–3.1	3.0–3.4	2.8–3.1	3.0–3.4	
C stock (t/ha)	93.5	147.7	135.4	105.8	120.6 ± 25.2
N stock (t/ha)	3.54	5.74	4.47	3.52	4.32 ± 1.05

535



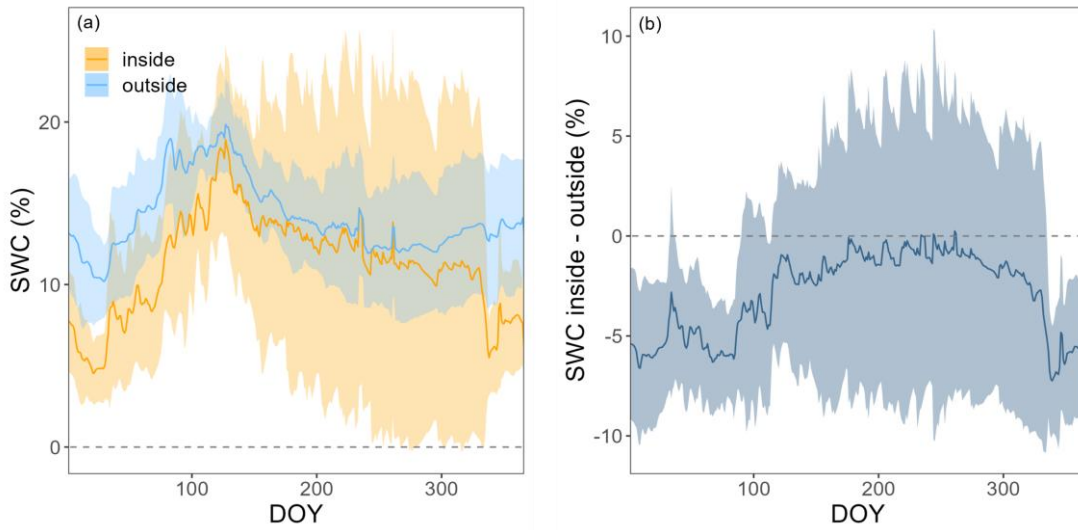
Fig. A.1: Picture of one of the automatic chambers (at location FF3).

540

Tests for chamber biases

We tested for chamber effects using SWC measurements from inside and outside FF1 and FF2 over all four years (Fig. A.2). SWC was highly variable over time as well as in space (Fig. A.2a). SWC differences between inside and outside the chamber varied between +10% and -10% during the four years (Fig. A.2b). No clear trend was detectable over time. The average difference between inside and outside SWC over the four years was $-2.9 \pm 5.8\%$. No significant differences in SWC inside vs. outside the chamber were detected during most of the year (exception: during winter, on average 5% lower SWC values inside compared to outside of the chamber). We found a high agreement in the dynamics of SWC inside and outside FF1 and FF2 (R^2 values of 0.69 and 0.82, respectively). In terms of T_{soil} , we did not find any significant differences inside vs. outside the chambers over most of the year (Fig. A.3a). The differences were only significantly different from zero in the months December, February, and March when T_{soil} inside the chambers was around 0.1-0.5 °C lower than outside the chambers (Fig. A.3b). At prevailing soil temperatures of around 0 °C in these months, such a difference in T_{soil} has no effect on the magnitude of forest-floor respiration (Fig. A.4).

550



555

Fig. A.2: a) Soil water content (SWC) at 5 cm inside (orange) and outside (light blue) and b) the difference in SWC at 5 cm between inside and outside the chambers FF1 and FF2 over the course of a year. Lines show means, bands show standard deviations over all four years.

560

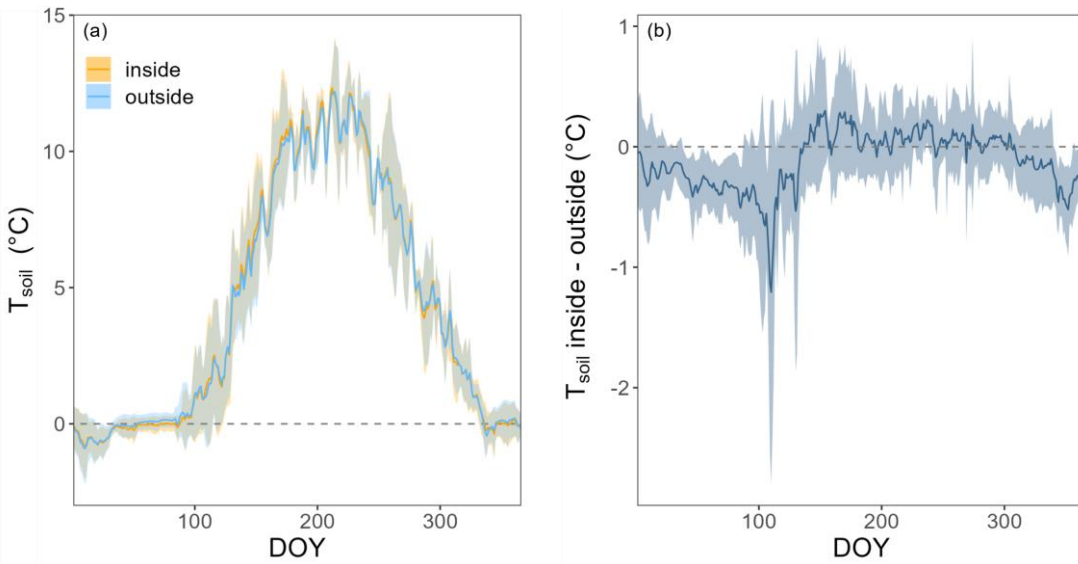


Fig. A.3: a) Soil temperatures (T_{soil}) at 5 cm inside (orange) and outside (light blue) and b) difference in T_{soil} at 5 cm between inside and outside of chambers (FF1 to FF4) over the course of a year. Lines show means, bands show standard deviations over three years (2017, 2020 and 2021).

565

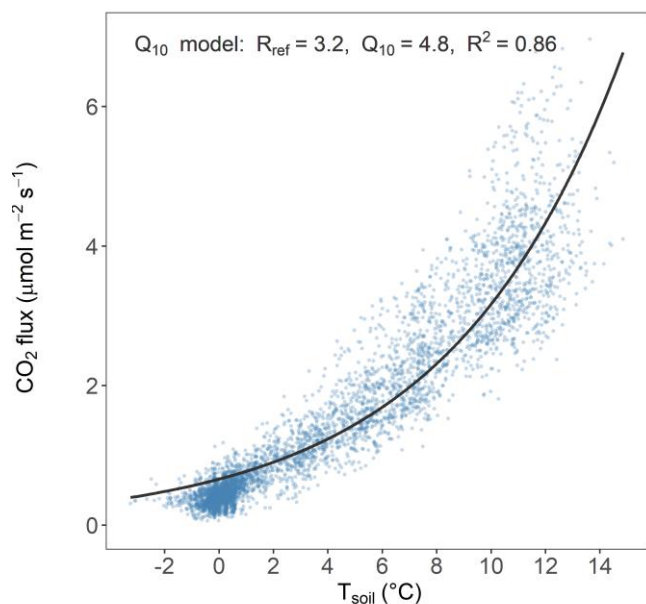


Fig. A.4: Q₁₀ model showing the relationship of daily means of T_{soil} at 5 cm and forest-floor respiration of all chambers and years.

570

Tab. A.3: Details of random forest models used for driver analysis and gap-filling for different time periods (entire year, separately for seasons). Number of observations used to train the models (training set), hyperparameters “mtry” and “ntree” as well as R² values for observed vs. predicted test data are given. “mtry” specifies how many variables were randomly sampled as candidates at each split, “ntree” indicates the number of trees.

Gas	Time period	No. observations in training set	mtry	ntree	test R ²
CO ₂	entire year	3111	10	2000	0.95
	spring	860	18	2000	0.94
	summer	623	14	2000	0.73
	autumn	836	14	2000	0.90
	winter	774	14	2000	0.63
CH ₄	entire year	2799	14	2000	0.87
	spring	825	18	2000	0.80
	summer	520	18	2000	0.76
	autumn	772	10	2000	0.72
	winter	674	10	2000	0.73

575

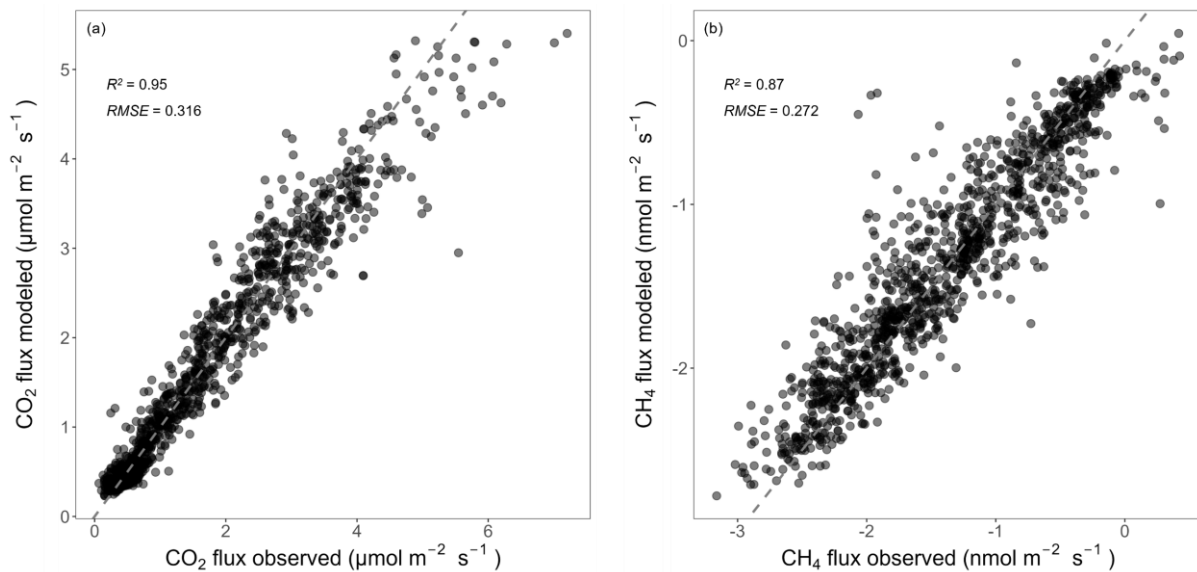


Fig. A.5: Relationships between observed and predicted forest-floor (a) respiration and (b) CH₄ fluxes from the RF models used for gap filling (only showing test data). R² and RSME are given. Black dashed lines mark the 1:1 lines.

580

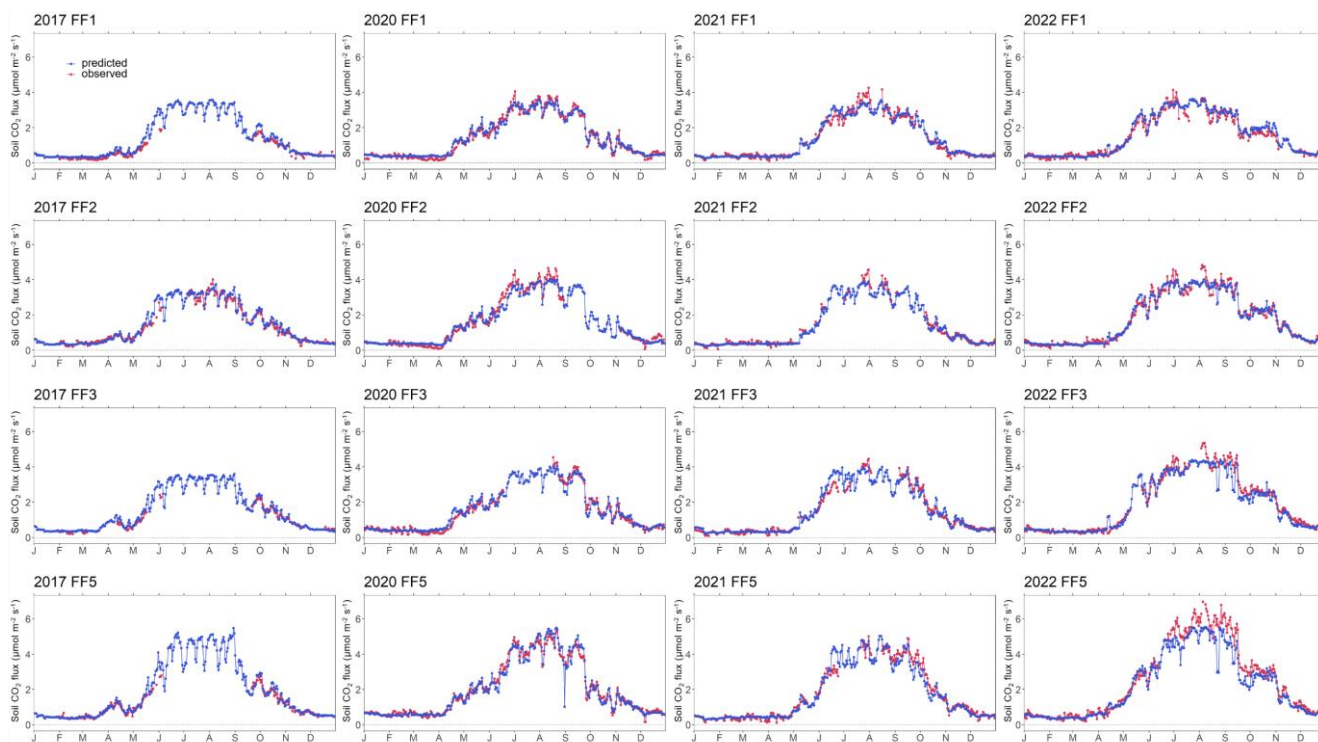


Fig. A.6: Time series of observed and predicted (using random forest model) forest-floor respiration fluxes for four years (2017, 2020–2022) and four chambers (FF1 to FF4).

585

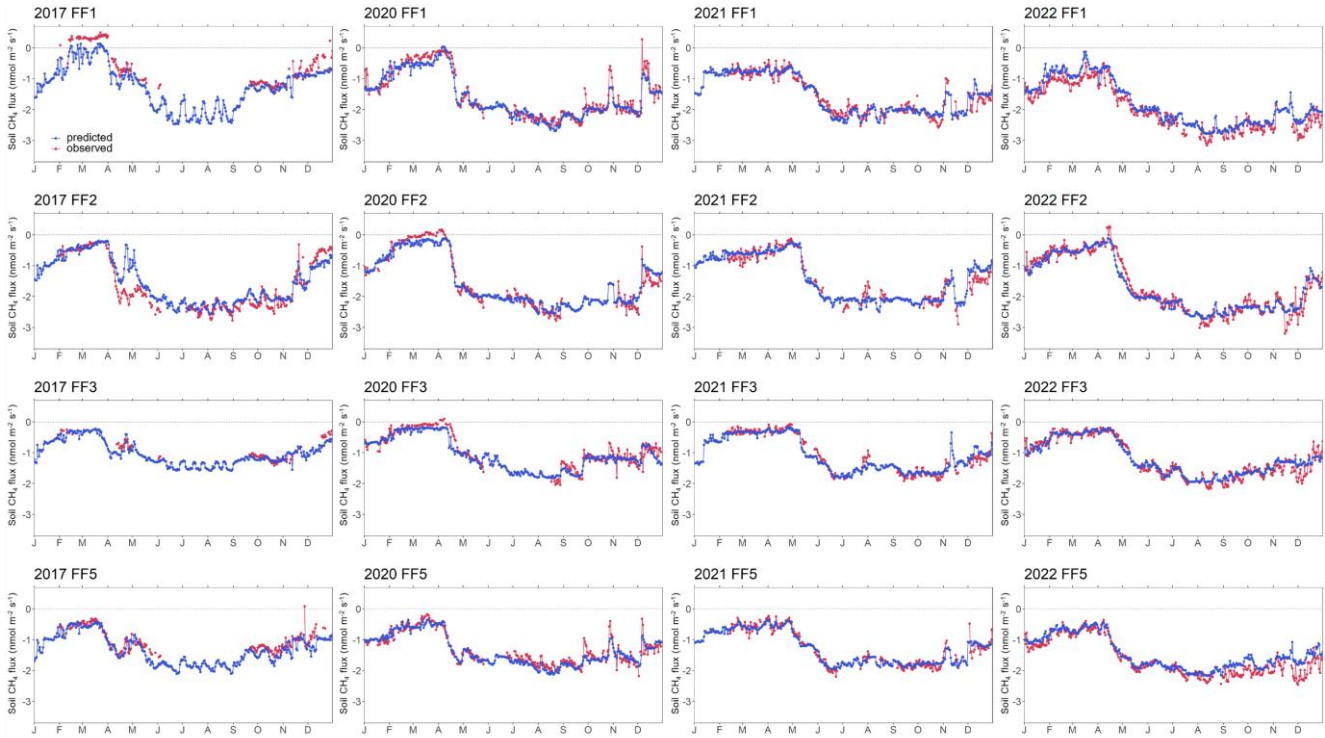


Fig. A.7: Time series of observed and predicted (using random forest model) forest-floor CH₄ fluxes for four years (2017, 2020–2022) and four chambers (FF1 to FF4).

590

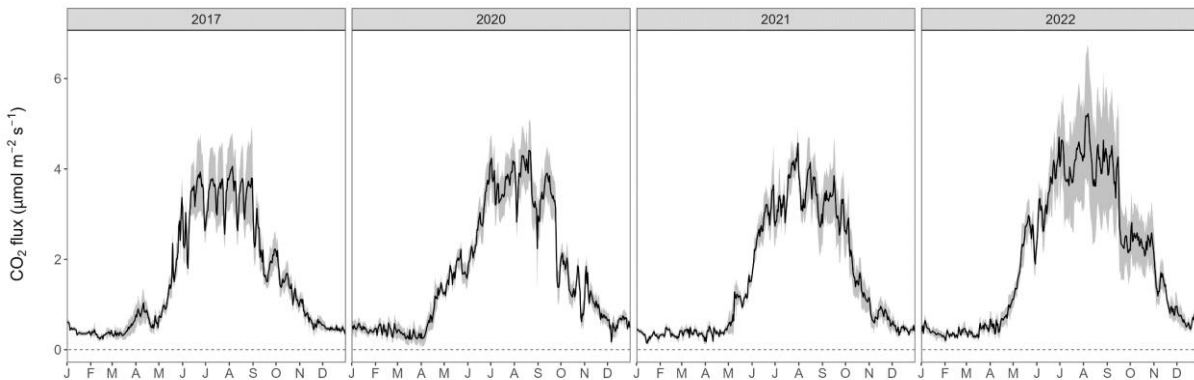


Fig. A.8: Gap-filled forest-floor respiration fluxes over four years (grey area: min-max among four chambers).

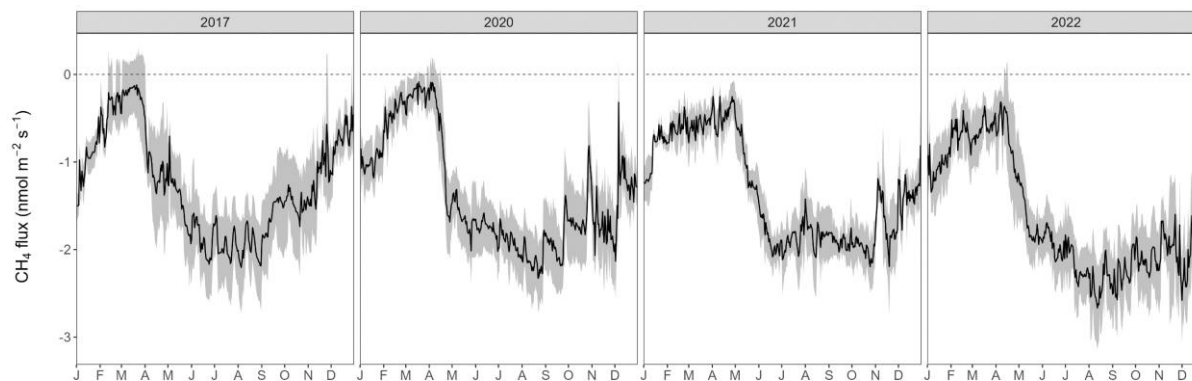


Fig. A.9: Gap-filled forest-floor CH₄ fluxes over four years (grey area: min-max among four chambers).

References

- Amthor, J. S.: The McCree–de Wit–Penning de Vries–Thornley Respiration Paradigms: 30 Years Later, *Ann. Bot.*, 86, 1–20, 600 <https://doi.org/10.1006/anbo.2000.1175>, 2000.
- Anjileli, H., Huning, L. S., Moftakhari, Ashraf, S., Asanjan, A. A., Norouzi, H., and AghaKouchak, A.: Extreme heat events heighten soil respiration, *Sci. Rep.*, 11, 6632, <https://doi.org/10.1038/s41598-021-85764-8>
- Arrouays, D., Saby, N. P. A., Boukir, H., Jolivet, C., Ratié, C., Schrumpp, M., Merbold, L., Gielen, B., Gogo, S., Delpierre, N., Vincent, G., Klumpp, K., and Loustau, D.: Soil sampling and preparation for monitoring soil carbon, *Int. Agrophysics*, 32, 605 633–643, <https://doi.org/10.1515/intag-2017-0047>, 2018.
- Barba, J., Cueva, A., Bahn, M., Barron-Gafford, G. A., Bond-Lamberty, B., Hanson, P. J., Jaimes, A., Kulmala, L., Pumpanen, J., Scott, R. L., Wohlfahrt, G., and Vargas, R.: Comparing ecosystem and soil respiration: Review and key challenges of tower-based and soil measurements, *Agric. For. Meteorol.*, 249, 434–443, <https://doi.org/10.1016/j.agrformet.2017.10.028>, 2018.
- Barba, J., Poyatos, R., and Vargas, R.: Automated measurements of greenhouse gases fluxes from tree stems and soils: 610 magnitudes, patterns and drivers, *Sci. Rep.*, 9, 4005, <https://doi.org/10.1038/s41598-019-39663-8>, 2019.
- Barrena, I., Menéndez, S., Duñabeitia, M., Merino, P., Florian Stange, C., Spott, O., González-Murua, C., and Estavillo, J. M.: Greenhouse gas fluxes (CO₂, N₂O and CH₄) from forest soils in the Basque Country: Comparison of different tree species and growth stages, *For. Ecol. Manag.*, 310, 600–611, <https://doi.org/10.1016/j.foreco.2013.08.065>, 2013.
- Barthel, M., Bauters, M., Baumgartner, S., Drake, T. W., Bey, N. M., Bush, G., Boeckx, P., Botefa, C. I., Dériaz, N., Ekamba, 615 G. L., Gallarotti, N., Mbayu, F. M., Mugula, J. K., Makelele, I. A., Mbongo, C. E., Mohn, J., Manda, J. Z., Mpambi, D. M., Ntaboba, L. C., Rukeza, M. B., Spencer, R. G. M., Summerauer, L., Vanlauwe, B., Van Oost, K., Wolf, B., and Six, J.: Low N₂O and variable CH₄ fluxes from tropical forest soils of the Congo Basin, *Nat. Commun.*, 13, 330, <https://doi.org/10.1038/s41467-022-27978-6>, 2022.

- 620 Basiliko, N., Knowles, R., and Moore, T. R.: Roles of moss species and habitat in methane consumption potential in a northern peatland, *Wetlands*, 24, 178–185, [https://doi.org/10.1672/0277-5212\(2004\)024\[0178:ROMSAH\]2.0.CO;2](https://doi.org/10.1672/0277-5212(2004)024[0178:ROMSAH]2.0.CO;2), 2004.
- Blankinship, J. C., McCorkle, E. P., Meadows, M. W., and Hart, S. C.: Quantifying the legacy of snowmelt timing on soil greenhouse gas emissions in a seasonally dry montane forest, *Glob. Change Biol.*, 24, 5933–5947, <https://doi.org/10.1111/gcb.14471>, 2018.
- 625 Bond-Lamberty, B., Bailey, V. L., Chen, M., Gough, C. M., and Vargas, R.: Globally rising soil heterotrophic respiration over recent decades, *Nature*, 560, 80–83, <https://doi.org/10.1038/s41586-018-0358-x>, 2018.
- Borken, W., Davidson, E. A., Savage, K., Sundquist, E. T., and Steudler, P.: Effect of summer throughfall exclusion, summer drought, and winter snow cover on methane fluxes in a temperate forest soil, *Soil Biol. Biochem.*, 38, 1388–1395, <https://doi.org/10.1016/j.soilbio.2005.10.011>, 2006.
- 630 [Braun, S., Schindler, C., and Rihm, B.: Growth trends of beech and Norway spruce in Switzerland: The role of nitrogen deposition, ozone, mineral nutrition and climate. *Sci. Total Environ.*, 599–600, 637–646, <https://doi.org/10.1016/j.scitotenv.2017.04.230>, 2017.](https://doi.org/10.1016/j.scitotenv.2017.04.230)
- Brümmer, C., Lyshede, B., Lempio, D., Delorme, J.-P., Rüffer, J. J., Fuß, R., Moffat, A. M., Hurkuck, M., Ibrom, A., Ambus, P., Flessa, H., and Kutsch, W. L.: Gas chromatography vs. quantum cascade laser-based N₂O flux measurements using a novel chamber design, *Biogeosciences*, 14, 1365–1381, <https://doi.org/10.5194/bg-14-1365-2017>, 2017.
- 635 Butterbach-Bahl, K., Baggs, E. M., Dannenmann, M., Kiese, R., and Zechmeister-Boltenstern, S.: Nitrous oxide emissions from soils: how well do we understand the processes and their controls?, *Philos. Trans. R. Soc. B Biol. Sci.*, 368, 20130122, <https://doi.org/10.1098/rstb.2013.0122>, 2013.
- CH2018: CH2018 – Climate Scenarios for Switzerland, Technical Report, National Centre for Climate Services, Zurich, 2018.
- 640 Chapuis-Lardy, L., Wrage, N., Metay, A., Chotte, J.-L., and Bernoux, M.: Soils, a sink for N₂O? A review, *Glob. Change Biol.*, 13, 1–17, <https://doi.org/10.1111/j.1365-2486.2006.01280.x>, 2007.
- Chen, W., Wang, S., Wang, J., Xia, J., Luo, Y., Yu, G., and Niu, S.: Evidence for widespread thermal optimality of ecosystem respiration, *Nat. Ecol. Evol.*, 7, 1379–1387, <https://doi.org/10.1038/s41559-023-02121-w>, 2023.
- Danielson, R. E. and Sutherland, P. L.: Porosity, in: *SSSA Book Series*, edited by: Klute, A., Soil Science Society of America, American Society of Agronomy, Madison, WI, USA, 443–461, <https://doi.org/10.2136/sssabookser5.1.2ed.c18>, 2018.
- 645 Davidson, E. A., Janssens, I. A., and Luo, Y.: On the variability of respiration in terrestrial ecosystems: moving beyond Q_{10} : On the variability of respiration in terrestrial ecosystems, *Glob. Change Biol.*, 12, 154–164, <https://doi.org/10.1111/j.1365-2486.2005.01065.x>, 2006.
- Debeer, D. and Strobl, C.: Conditional permutation importance revisited, *BMC Bioinformatics*, 21, 307, <https://doi.org/10.1186/s12859-020-03622-2>, 2020.
- 650 Debeer, D., Hothorn, T., and Strobl, C.: permimp: Conditional Permutation Importance, 2021.
- Dutaur, L. and Verchot, L. V.: A global inventory of the soil CH₄ sink, *Glob. Biogeochem. Cycles*, 21, GB4013, <https://doi.org/10.1029/2006GB002734>, 2007.

- 655 Fest, B. J., Livesley, S. J., Drösler, M., van Gorsel, E., and Arndt, S. K.: Soil–atmosphere greenhouse gas exchange in a cool, temperate *Eucalyptus delegatensis* forest in south-eastern Australia, *Agric. For. Meteorol.*, 149, 393–406, <https://doi.org/10.1016/j.agrformet.2008.09.007>, 2009.
- 660 Friedlingstein, P., O’Sullivan, M., Jones, M. W., Andrew, R. M., Bakker, D. C. E., Hauck, J., Landschützer, P., Le Quééré, C., Luijkx, I. T., Peters, G. P., Peters, W., Pongratz, J., Schwingshackl, C., Sitch, S., Canadell, J. G., Ciais, P., Jackson, R. B., Alin, S. R., Anthoni, P., Barbero, L., Bates, N. R., Becker, M., Bellouin, N., Decharme, B., Bopp, L., Brasika, I. B. M., Cadule, P., Chamberlain, M. A., Chandra, N., Chau, T.-T.-T., Chevallier, F., Chini, L. P., Cronin, M., Dou, X., Enyo, K., Evans, W., Falk, S., Feely, R. A., Feng, L., Ford, D. J., Gasser, T., Ghattas, J., Gkritzalis, T., Grassi, G., Gregor, L., Gruber, N., Gürses, Ö., Harris, I., Hefner, M., Heinke, J., Houghton, R. A., Hurtt, G. C., Iida, Y., Ilyina, T., Jacobson, A. R., Jain, A., Jarníková, T., Jersild, A., Jiang, F., Jin, Z., Joos, F., Kato, E., Keeling, R. F., Kennedy, D., Klein Goldewijk, K., Knauer, J., Korsbakken, J. I., Körtzinger, A., Lan, X., Lefèvre, N., Li, H., Liu, J., Liu, Z., Ma, L., Marland, G., Mayot, N., McGuire, P. C., McKinley, G. A., Meyer, G., Morgan, E. J., Munro, D. R., Nakaoka, S.-I., Niwa, Y., O’Brien, K. M., Olsen, A., Omar, A. M., Ono, T., 665 Paulsen, M., Pierrot, D., Pockock, K., Poulter, B., Powis, C. M., Rehder, G., Resplandy, L., Robertson, E., Rödenbeck, C., Rosan, T. M., Schwinger, J., Séférian, R., et al.: Global Carbon Budget 2023, *Earth Syst. Sci. Data*, 15, 5301–5369, <https://doi.org/10.5194/essd-15-5301-2023>, 2023.
- 670 Fuentes, S., Palmer, A. R., Taylor, D., Zeppel, M., Whitley, R., and Eamus, D.: An automated procedure for estimating the leaf area index (LAI) of woodland ecosystems using digital imagery, MATLAB programming and its application to an examination of the relationship between remotely sensed and field measurements of LAI, *Funct. Plant Biol.*, 35, 1070, <https://doi.org/10.1071/FP08045>, 2008.
- Gao, D., Hagedorn, F., Zhang, L., Liu, J., Qu, G., Sun, J., Peng, B., Fan, Z., Zheng, J., Jiang, P., and Bai, E.: Small and transient response of winter soil respiration and microbial communities to altered snow depth in a mid-temperate forest, *Appl. Soil Ecol.*, 130, 40–49, <https://doi.org/10.1016/j.apsoil.2018.05.010>, 2018.
- 675 Gaumont-Guay, D., Black, T. A., Barr, A. G., Griffis, T. J., Jassal, R. S., Krishnan, P., Grant, N., and Nesic, Z.: Eight years of forest-floor CO₂ exchange in a boreal black spruce forest: Spatial integration and long-term temporal trends, *Agric. For. Meteorol.*, 184, 25–35, <https://doi.org/10.1016/j.agrformet.2013.08.010>, 2014.
- 680 Gharun, M., Klesse, S., Tomlinson, G., Waldner, P., Stocker, B., Rihm, B., Siegwolf, R., and Buchmann, N.: Effect of nitrogen deposition on centennial forest water-use efficiency, *Environ. Res. Lett.*, 16, 114036, <https://doi.org/10.1088/1748-9326/ac30f9>, 2021.
- Goldberg, S. D. and Gebauer, G.: N₂O and NO fluxes between a Norway spruce forest soil and atmosphere as affected by prolonged summer drought, *Soil Biol.*, 41, 1986–1995, <https://doi.org/10.1016/j.soilbio.2009.07.001>, 2009.
- 685 Goldberg, S. D., Borken, W., and Gebauer, G.: N₂O emission in a Norway spruce forest due to soil frost: concentration and isotope profiles shed a new light on an old story, *Biogeochemistry*, 97, 21–30, <https://doi.org/10.1007/s10533-009-9294-z>, 2010.
- Goldman, M. B., Groffman, P. M., Pouyat, R. V., McDonnell, M. J., and Pickett, S. T. A.: CH₄ uptake and N availability in forest soils along an urban to rural gradient, *Soil Biol. Biochem.*, 27, 281–286, [https://doi.org/10.1016/0038-0717\(94\)00185-4](https://doi.org/10.1016/0038-0717(94)00185-4), 1995.
- 690 Goldstein, A., Kapelner, A., Bleich, J., and Pitkin, E.: Peeking inside the black box: Visualizing statistical learning with plots of individual conditional expectation, *J. Comput. Graph. Stat.*, 24, 44–65, <https://doi.org/10.1080/10618600.2014.907095>, 2015.

- Greenwell, B., M.: pdp: An R package for constructing partial dependence plots, *R J.*, 9, 421, <https://doi.org/10.32614/RJ-2017-016>, 2017.
- 695 Groffman, P. M., Hardy, J. P., Driscoll, C. T., and Fahey, T. J.: Snow depth, soil freezing, and fluxes of carbon dioxide, nitrous oxide and methane in a northern hardwood forest, *Glob. Change Biol.*, 12, 1748–1760, <https://doi.org/10.1111/j.1365-2486.2006.01194.x>, 2006.
- Guo, C., Zhang, L., Li, S., Li, Q., and Dai, G.: Comparison of Soil Greenhouse Gas Fluxes during the Spring Freeze–Thaw Period and the Growing Season in a Temperate Broadleaved Korean Pine Forest, Changbai Mountains, China, *Forests*, 11, 1135, 2020.
- 700 Hahn, M., Gartner, K., and Zechmeister-Boltenstern, S.: Greenhouse gas emissions (N₂O, CO₂ and CH₄) from three forest soils near Vienna (Austria) with different water and nitrogen regimes, *Bodenkultur*, 51, 115–125, 2000.
- Hanson, P. J., Edwards, N. T., Garten, C. T., and Andrews, J. A.: Separating root and soil microbial contributions to soil respiration: A review of methods and observations, *Biogeochemistry*, 48, 115–146, <https://doi.org/10.1023/A:1006244819642>, 2000.
- 705 [Heinzle, J., Kitzler, B., Zechmeister-Boltenstern, S., Tian, Y., Kwatcho Kengdo, S., Wanek, W., Borken, W., and Schindlbacher, A.: Soil CH₄ and N₂O response diminishes during decadal soil warming in a temperate mountain forest, *Agric. For. Meteorol.*, 329, 109287, <https://doi.org/10.1016/j.agrformet.2022.109287>, 2023.](https://doi.org/10.1016/j.agrformet.2022.109287)
- [Hettelingh, J. P., Posch, M., and Slootweg, J.: European critical loads: database, biodiversity and ecosystems at risk : CCE Final Report 2017, Rijksinstituut voor Volksgezondheid en Milieu, Bilthoven, Netherlands, 2017.](https://www.cce.nl/publications/2017/01/hettelingh-et-al-2017-european-critical-loads-database-biodiversity-and-ecosystems-at-risk)
- 710 Högberg, P., Nordgren, A., Buchmann, N., Taylor, A. F. S., Ekblad, A., Högberg, M. N., Nyberg, G., Ottosson-Löfvenius, M., and Read, D. J.: Large-scale forest girdling shows that current photosynthesis drives soil respiration, *Nature*, 411, 789–792, <https://doi.org/10.1038/35081058>, 2001.
- Hopfensperger, K. N., Gault, C. M., and Groffman, P. M.: Influence of plant communities and soil properties on trace gas fluxes in riparian northern hardwood forests, *For. Ecol. Manag.*, 258, 2076–2082, <https://doi.org/10.1016/j.foreco.2009.08.004>, 2009.
- 715 Hutchinson, G. L. and Mosier, A. R.: Improved Soil Cover Method for Field Measurement of Nitrous Oxide Fluxes, *Soil Sci. Soc. Am. J.*, 45, 311–316, <https://doi.org/10.2136/sssaj1981.03615995004500020017x>, 1981.
- Ingestad, T.: Studies on the Nutrition of Forest Tree Seedlings. II Mineral Nutrition of Spruce, *Physiol. Plant.*, 568–593, 1959.
- 720 IPCC: Climate Change 2021: The Physical Science Basis. Contribution of Working Group I to the Sixth Assessment Report of the Intergovernmental Panel on Climate Change, Cambridge University Press, Cambridge, United Kingdom and New York, NY, USA, 2021.
- 725 Janssens, I. A., Lankreijer, H., Matteucci, G., Kowalski, A. S., Buchmann, N., Epron, D., Pilegaard, K., Kutsch, W., Longdoz, B., Grünwald, T., Montagnani, L., Dore, S., Rebmann, C., Moors, E. J., Grelle, A., Rannik, Ü., Morgenstern, K., Oltchev, S., Clement, R., Guðmundsson, J., Minerbi, S., Berbigier, P., Ibrom, A., Moncrieff, J., Aubinet, M., Bernhofer, C., Jensen, N. O., Vesala, T., Granier, A., Schulze, E.-D., Lindroth, A., Dolman, A. J., Jarvis, P. G., Ceulemans, R., and Valentini, R.: Productivity overshadows temperature in determining soil and ecosystem respiration across European forests, *Glob. Change Biol.*, 7, 269–278, <https://doi.org/10.1046/j.1365-2486.2001.00412.x>, 2001.

Jörg, S.: Böden im Seehornwald bei Davos und deren Vorrat an Kohlenstoff und Stickstoff. Diplomarbeit, Zürcher Hochschule für Angewandte Wissenschaften, Zürcher Hochschule für Angewandte Wissenschaften, Zurich, 79 pp., 2008.

730 Kim, Y., Kodama, Y., and Fochesatto, G. J.: Environmental factors regulating winter CO₂ flux in snow-covered black forest soil of Interior Alaska, *Geochem. J.*, 51, 359–371, <https://doi.org/10.2343/geochemj.2.0475>, 2017.

Klein, G., Vitasse, Y., Rixen, C., Marty, C., and Rebetez, M.: Shorter snow cover duration since 1970 in the Swiss Alps due to earlier snowmelt more than to later snow onset, *Clim. Change*, 139, 637–649, <https://doi.org/10.1007/s10584-016-1806-y>, 2016.

735 Krause, K., Niklaus, P. A., and Schleppei, P.: Soil-atmosphere fluxes of the greenhouse gases CO₂, CH₄ and N₂O in a mountain spruce forest subjected to long-term N addition and to tree girdling, *Agric. For. Meteorol.*, 181, 61–68, <https://doi.org/10.1016/j.agrformet.2013.07.007>, 2013.

Kuhn, M.: Building Predictive Models in R Using the caret Package, *J. Stat. Softw.*, 28, 1–26, <https://doi.org/10.18637/jss.v028.i05>, 2008.

740 Lembrechts, J. J., van den Hoogen, J., Aalto, J., Ashcroft, M. B., De Frenne, P., Kemppinen, J., Kopecký, M., Luoto, M., Maclean, I. M. D., Crowther, T. W., Bailey, J. J., Haesen, S., Klinges, D. H., Niittynen, P., Scheffers, B. R., Van Meerbeek, K., Aartsma, P., Abdalaze, O., Abedi, M., Aerts, R., Ahmadian, N., Ahrends, A., Alatalo, J. M., Alexander, J. M., Allonsius, C. N., Altman, J., Ammann, C., Andres, C., Andrews, C., Ardö, J., Arriga, N., Arzac, A., Aschero, V., Assis, R. L., Assmann, J. J., Bader, M. Y., Bahalkheh, K., Barančok, P., Barrio, I. C., Barros, A., Barthel, M., Basham, E. W., Bauters, M., Bazzichetto, M., Marchesini, L. B., Bell, M. C., Benavides, J. C., Benito Alonso, J. L., Berauer, B. J., Bjerke, J. W., Björk, R. G., Björkman, M. P., Björnsdóttir, K., Blonder, B., Boeckx, P., Boike, J., Bokhorst, S., Brum, B. N. S., Brúna, J., Buchmann, N., Buysse, P., Camargo, J. L., Campoe, O. C., Candan, O., Canessa, R., Cannone, N., Carbognani, M., Carnicer, J., Casanova-Katny, A., Cesarz, S., Chojnicki, B., Choler, P., Chown, S. L., Cifuentes, E. F., Čiliak, M., Contador, T., Convey, P., Cooper, E. J., Cremonese, E., Curasi, S. R., Curtis, R., Cutini, M., Dahlberg, C. J., Daskalova, G. N., de Pablo, M. A., Della Chiesa, S., 750 Dengler, J., Deronde, B., Descombes, P., Di Cecco, V., Di Musciano, M., Dick, J., Dimarco, R. D., Dolezal, J., Dorrepaal, E., Dušek, J., Eisenhauer, N., Eklundh, L., Erickson, T. E., et al.: Global maps of soil temperature, *Glob. Change Biol.*, 28, 3110–3144, <https://doi.org/10.1111/gcb.16060>, 2022.

Liu, S., Schloter, M., and Brüggemann, N.: Accumulation of NO₂⁻ during periods of drying stimulates soil N₂O emissions during subsequent rewetting: Nitrite stimulates N₂O emissions during rewetting, *Eur. J. Soil Sci.*, 69, 936–946, <https://doi.org/10.1111/ejss.12683>, 2018.

Luedeling, E. and Fernandez, E.: chillR: Statistical methods for phenology analysis in temperate fruit, 2022.

Luo, G. J., Brüggemann, N., Wolf, B., Gasche, R., Grote, R., and Butterbach-Bahl, K.: Decadal variability of soil CO₂, NO, N₂O, and CH₄ fluxes at the Höglwald Forest, Germany, *Biogeosciences*, 9, 1741–1763, <https://doi.org/10.5194/BG-9-1741-2012>, 2011.

760 Luo, G. J., Kiese, R., Wolf, B., and Butterbach-Bahl, K.: Effects of soil temperature and moisture on methane uptake and nitrous oxide emissions across three different ecosystem types, *Biogeosciences*, 10, 3205–3219, <https://doi.org/10.5194/bg-10-3205-2013>, 2013.

Martins, C. S. C., Nazaries, L., Delgado-Baquerizo, M., Macdonald, C. A., Anderson, I. C., Hobbie, S. E., Venterea, R. T., Reich, P. B., and Singh, B. K.: Identifying environmental drivers of greenhouse gas emissions under warming and reduced rainfall in boreal–temperate forests, *Funct. Ecol.*, 31, 2356–2368, <https://doi.org/10.1111/1365-2435.12928>, 2017.

765

- Martinson, G. O., Müller, A. K., Matson, A. L., Corre, M. D., and Veldkamp, E.: Nitrogen and Phosphorus Control Soil Methane Uptake in Tropical Montane Forests, *J. Geophys. Res. Biogeosciences*, 126(8), e2020JG005970, <https://doi.org/10.1029/2020JG005970>, 2021.
- 770 McManus, J. B., Nelson, D. D., Herndon, S. C., Shorter, J. H., Zahniser, M. S., Blaser, S., Hvozدارa, L., Muller, A., Giovannini, M., and Faist, J.: Comparison of cw and pulsed operation with a TE-cooled quantum cascade infrared laser for detection of nitric oxide at 1900 cm⁻¹, *Appl. Phys. B*, 85, 235–241, <https://doi.org/10.1007/s00340-006-2407-7>, 2006.
- Mitra, B., Miao, G., Minick, K., McNulty, S. G., Sun, G., Gavazzi, M., King, J. S., and Noormets, A.: Disentangling the Effects of Temperature, Moisture, and Substrate Availability on Soil CO₂ Efflux, *J. Geophys. Res. Biogeosciences*, 124, 2060–2075, <https://doi.org/10.1029/2019JG005148>, 2019.
- 775 Ni, X. and Groffman, P. M.: Declines in methane uptake in forest soils, *Proc. Natl. Acad. Sci.*, 115, 8587–8590, <https://doi.org/10.1073/pnas.1807377115>, 2018.
- Nissan, A., Alcolombri, U., Peleg, N., Galili, N., Jimenez-Martinez, J., Molnar, P., and Holzner, M.: Global warming accelerates soil heterotrophic respiration, *Nat. Commun.*, 14, 3452, <https://doi.org/10.1038/s41467-023-38981-w>, 2023.
- 780 Pang, J., Peng, C., Wang, X., Zhang, H., and Zhang, S.: Soil-atmosphere exchange of carbon dioxide, methane and nitrous oxide in temperate forests along an elevation gradient in the Qinling Mountains, China, *Plant Soil*, 488, 325–342, <https://doi.org/10.1007/s11104-023-05967-y>, 2023.
- Papen, H. and Butterbach-Bahl, K.: A 3-year continuous record of nitrogen trace gas fluxes from untreated and limed soil of a N-saturated spruce and beech forest ecosystem in Germany: 1. N₂O emissions, *J. Geophys. Res. Atmospheres*, 104, 18487–18503, <https://doi.org/10.1029/1999JD900293>, 1999.
- 785 Pavelka, M., Acosta, M., Kiese, R., Altimir, N., Brümmner, C., Crill, P., Darenova, E., Fuß, R., Gielen, B., Graf, A., Klemetsson, L., Lohila, A., Longdoz, B., Lindroth, A., Nilsson, M., Jiménez, S. M., Merbold, L., Montagnani, L., Peichl, M., Pihlatie, M., Pumpanen, J., Ortiz, P. S., Silvennoinen, H., Skiba, U., Vestin, P., Weslien, P., Janous, D., and Kutsch, W.: Standardisation of chamber technique for CO₂, N₂O and CH₄ fluxes measurements from terrestrial ecosystems, *Int. Agrophysics*, 32, 569–587, <https://doi.org/10.1515/intag-2017-0045>, 2018.
- 790 Pilegaard, K., Mikkelsen, T. N., Beier, C., Jensen, N., Ambus, P., and Ro-Poulsen, H.: Field measurements of atmosphere–biosphere interactions in a Danish beech forest, *Boreal Environ. Res.*, 8, 315–333, 2003.
- R Core Team: R: A language and environment for statistical computing, R Foundation for Statistical Computing, Vienna, Austria, 2022.
- 795 Reichstein, M., Bahn, M., Ciais, P., Frank, D., Mahecha, M. D., Seneviratne, S. I., Zscheischler, J., Beer, C., Buchmann, N., Frank, D. C., Papale, D., Rammig, A., Smith, P., Thonicke, K., van der Velde, M., Vicca, S., Walz, A., and Wattenbach, M.: Climate extremes and the carbon cycle, *Nature*, 500, 287–295, <https://doi.org/10.1038/nature12350>, 2013.
- Reinmann, A. B. and Templer, P. H.: Increased soil respiration in response to experimentally reduced snow cover and increased soil freezing in a temperate deciduous forest, *Biogeochemistry*, 140, 359–371, <https://doi.org/10.1007/s10533-018-0497-z>, 2018.
- 800 Richardson, A. D., Hollinger, D. Y., Shoemaker, J. K., Hughes, H., Savage, K., and Davidson, E. A.: Six years of ecosystem-atmosphere greenhouse gas fluxes measured in a sub-boreal forest, *Sci. Data*, 6, 117, <https://doi.org/10.1038/s41597-019-0119-1>, 2019.

- Robette, N.: *moreparty*: A toolbox for conditional inference trees and random forests, 2023.
- 805 Ruehr, N. K., Knohl, A., and Buchmann, N.: Environmental variables controlling soil respiration on diurnal, seasonal and annual time-scales in a mixed mountain forest in Switzerland, *Biogeochemistry*, 98, 153–170, <https://doi.org/10.1007/s10533-009-9383-z>, 2010.
- Rütting, T., Björnsne, A.-K., Weslien, P., Kasimir, Å., and Klemedtsson, L.: Low Nitrous Oxide Emissions in a Boreal Spruce Forest Soil, Despite Long-Term Fertilization, *Front. For. Glob. Change*, 4, <https://doi.org/10.3389/ffgc.2021.710574>, 2021.
- 810 Saby, N., Loubet, B., Goydarag, M. G., Papale, D., Arrouays, D., and Lafont, S.: Computing C Stock for one ICOS Site, ICOS Ecosystem Thematic Centre, 2023.
- 815 Saunois, M., Stavert, A. R., Poulter, B., Bousquet, P., Canadell, J. G., Jackson, R. B., Raymond, P. A., Dlugokencky, E. J., Houweling, S., Patra, P. K., Ciais, P., Arora, V. K., Bastviken, D., Bergamaschi, P., Blake, D. R., Brailsford, G., Bruhwiler, L., Carlson, K. M., Carrol, M., Castaldi, S., Chandra, N., Crevoisier, C., Crill, P. M., Covey, K., Curry, C. L., Etiope, G., Frankenberg, C., Gedney, N., Hegglin, M. I., Höglund-Isaksson, L., Hugelius, G., Ishizawa, M., Ito, A., Janssens-Maenhout, G., Jensen, K. M., Joos, F., Kleinen, T., Krummel, P. B., Langenfelds, R. L., Laruelle, G. G., Liu, L., Machida, T., Maksyutov, S., McDonald, K. C., McNorton, J., Miller, P. A., Melton, J. R., Morino, I., Müller, J., Murguia-Flores, F., Naik, V., Niwa, Y., Noce, S., O'Doherty, S., Parker, R. J., Peng, C., Peng, S., Peters, G. P., Prigent, C., Prinn, R., Ramonet, M., Regnier, P., Riley, W. J., Rosentreter, J. A., Segers, A., Simpson, I. J., Shi, H., Smith, S. J., Steele, L. P., Thornton, B. F., Tian, H., Tohjima, Y., Tubiello, F. N., Tsuruta, A., Viovy, N., Voulgarakis, A., Weber, T. S., van Weele, M., van der Werf, G. R., Weiss, R. F., 820 Worthy, D., Wunch, D., Yin, Y., Yoshida, Y., Zhang, W., Zhang, Z., Zhao, Y., Zheng, B., Zhu, Q., Zhu, Q., and Zhuang, Q.: The Global Methane Budget 2000–2017, *Earth Syst. Sci. Data*, 12, 1561–1623, <https://doi.org/10.5194/essd-12-1561-2020>, 2020.
- Schaufler, G., Kitzler, B., Schindlbacher, A., Skiba, U., Sutton, M., and Zechmeister-Boltenstern, S.: Greenhouse gas emissions from European soils under different land use: effects of soil moisture and temperature, *Eur. J. Soil Sci.*, 61, 683–825 696, <https://doi.org/10.1111/j.1365-2389.2010.01277.x>, 2010.
- Schindlbacher, A., Zechmeister-Boltenstern, S., Glatzel, G., and Jandl, R.: Winter soil respiration from an Austrian mountain forest, *Agric. For. Meteorol.*, 146, 205–215, <https://doi.org/10.1016/j.agrformet.2007.06.001>, 2007.
- Schindlbacher, A., Jandl, R., and Schindlbacher, S.: Natural variations in snow cover do not affect the annual soil CO₂ from a mid-elevation temperate forest, *Glob. Change Biol.*, 20, 622–632, <https://doi.org/10.1111/gcb.12367>, 2014.
- 830 Schulze, E.-D. (Ed.)Caldwell, M. M., Heldmaier, G., Lange, O. L., Mooney, H. A., Schulze, E.-D., and Sommer, U.: *Carbon and Nitrogen Cycling in European Forest Ecosystems*, Springer Berlin Heidelberg, Berlin, Heidelberg, <https://doi.org/10.1007/978-3-642-57219-7>, 2000.
- 835 Scott-Denton, L. E., Rosenstiel, T. N., and Monson, R. K.: Differential controls by climate and substrate over the heterotrophic and rhizospheric components of soil respiration: Controls over soil respiration, *Glob. Change Biol.*, 12, 205–216, <https://doi.org/10.1111/j.1365-2486.2005.01064.x>, 2006.
- Sommerfeld, R. A., Mosier, A. R., and Musselman, R. C.: CO₂, CH₄ and N₂O flux through a Wyoming snowpack and implications for global budgets, *Nature*, 361, 140–142, <https://doi.org/10.1038/361140a0>, 1993.
- Song, Y., Zou, Y., Wang, G., and Yu, X.: Altered soil carbon and nitrogen cycles due to the freeze-thaw effect: A meta-analysis, *Soil Biol. Biochem.*, 109, 35–49, <https://doi.org/10.1016/j.soilbio.2017.01.020>, 2017.

- 840 Strobl, C., Boulesteix, A.-L., Zeileis, A., and Hothorn, T.: Bias in random forest variable importance measures: Illustrations, sources and a solution, *BMC Bioinformatics*, 8, 25, <https://doi.org/10.1186/1471-2105-8-25>, 2007.
- Strobl, C., Boulesteix, A.-L., Kneib, T., Augustin, T., and Zeileis, A.: Conditional variable importance for random forests, *BMC Bioinformatics*, 9, 307, <https://doi.org/10.1186/1471-2105-9-307>, 2008.
- 845 Thimonier, A., Graf Pannatier, E., Schmitt, M., Waldner, P., Walthert, L., Schleppei, P., Dobbertin, M., and Kräuchi, N.: Does exceeding the critical loads for nitrogen alter nitrate leaching, the nutrient status of trees and their crown condition at Swiss Long-term Forest Ecosystem Research (LWF) sites?, *Eur. J. For. Res.*, 443–461, <https://doi.org/10.1007/s10342-009-0328-9>, 2010.
- 850 Thimonier, A., Kosonen, Z., Braun, S., Rihm, B., Schleppei, P., Schmitt, M., Seitler, E., Waldner, P., and Thöni, L.: Total deposition of nitrogen in Swiss forests: comparison of assessment methods and evaluation of changes over two decades, *Atmos. Environ.*, 335–350, <https://doi.org/10.1016/j.atmosenv.2018.10.051>, 2019.
- Tschopp, T.: Zur Geschichte des Seehornwaldes in Davos. Praktikumsarbeit, WSL, Birmensdorf, 2012.
- Ueyama, M., Takeuchi, R., Takahashi, Y., Ide, R., Ataka, M., Kosugi, Y., Takahashi, K., and Saigusa, N.: Methane uptake in a temperate forest soil using continuous closed-chamber measurements, *Agric. For. Meteorol.*, 213, 1–9, <https://doi.org/10.1016/j.agrformet.2015.05.004>, 2015.
- 855 Ullah, S., Frasier, R., Pelletier, L., and Moore, T. R.: Greenhouse gas fluxes from boreal forest soils during the snow-free period in Quebec, Canada, *Can. J. For. Res.*, 39, 666–680, <https://doi.org/10.1139/X08-209>, 2009.
- Von Arnold, K., Weslien, P., Nilsson, M., Svensson, B. H., and Klemetsson, L.: Fluxes of CO₂, CH₄ and N₂O from drained coniferous forests on organic soils, *For. Ecol. Manag.*, 210, 239–254, <https://doi.org/10.1016/j.foreco.2005.02.031>, 2005.
- 860 Wang, C., Han, Y., Chen, J., Wang, X., Zhang, Q., and Bond-Lamberty, B.: Seasonality of soil CO₂ efflux in a temperate forest: Biophysical effects of snowpack and spring freeze–thaw cycles, *Agric. For. Meteorol.*, 177, 83–92, <https://doi.org/10.1016/j.agrformet.2013.04.008>, 2013.
- [Wang, Y.-R., Buchmann, N., Hessen, D. O., Stordal, F., Erisman, J. W., Vollsnes, A. V., Andersen, T., and Dolman, H.: Disentangling effects of natural and anthropogenic drivers on forest net ecosystem production, *Sci. Total Environ.*, 839, 156326, <https://doi.org/10.1016/j.scitotenv.2022.156326>, 2022.](https://doi.org/10.1016/j.scitotenv.2022.156326)
- 865 Wen, Y., Corre, M. D., Schrell, W., and Veldkamp, E.: Gross N₂O emission and gross N₂O uptake in soils under temperate spruce and beech forests, *Soil Biol. Biochem.*, 112, 228–236, <https://doi.org/10.1016/j.soilbio.2017.05.011>, 2017.
- Wu, X., Zang, S., Ma, D., Ren, J., Chen, Q., and Dong, X.: Emissions of CO₂, CH₄, and N₂O Fluxes from Forest Soil in Permafrost Region of Daxing’an Mountains, Northeast China, *Int. J. Environ. Res. Public Health*, 16, 2999, <https://doi.org/10.3390/ijerph16162999>, 2019.
- 870 Xie, J., Kneubühler, M., Garonna, I., Notarnicola, C., De Gregorio, L., De Jong, R., Chimani, B., and Schaepman, M. E.: Altitude-dependent influence of snow cover on alpine land surface phenology: Snow cover and Alpine phenology, *J. Geophys. Res. Biogeosciences*, 122, 1107–1122, <https://doi.org/10.1002/2016JG003728>, 2017.
- Xu, Z., Zhou, F., Yin, H., and Liu, Q.: Winter soil CO₂ efflux in two contrasting forest ecosystems on the eastern Tibetan Plateau, China, *J. For. Res.*, 26, 679–686, <https://doi.org/10.1007/s11676-015-0120-2>, 2015.

- 875 Yu, L., Huang, Y., Zhang, W., Li, T., and Sun, W.: Methane uptake in global forest and grassland soils from 1981 to 2010, *Sci. Total Environ.*, 607–608, 1163–1172, <https://doi.org/10.1016/j.scitotenv.2017.07.082>, 2017.
- Yuste, J. C., Nagy, M., Janssens, I. A., Carrara, A., and Ceulemans, R.: Soil respiration in a mixed temperate forest and its contribution to total ecosystem respiration, *Tree Physiol.*, 25, 609–619, <https://doi.org/10.1093/treephys/25.5.609>, 2005.
- 880 Zielis, S., Etzold, S., Zweifel, R., Eugster, W., Haeni, M., and Buchmann, N.: NEP of a Swiss subalpine forest is significantly driven not only by current but also by previous year's weather, *Biogeosciences*, 11, 1627–1635, <https://doi.org/10.5194/bg-11-1627-2014>, 2014.